A NEAR-SURFACE GEOPHYSICAL INVESTIGATION OF THE EFFECTS OF MEASURED AND REPEATED REMOVAL OF OVERLYING SOIL ON INSTRUMENT RESPONSE

A Thesis

by

ZACHARY RYAN LONG

Submitted to the Office of Graduate Studies of
Texas A&M University
in partial fulfillment of the requirements for the degree of

MASTER OF SCIENCE

August 2005

Major Subject: Geophysics

A NEAR-SURFACE GEOPHYSICAL INVESTIGATION OF THE EFFECTS OF MEASURED AND REPEATED REMOVAL OF OVERLYING SOIL ON INSTRUMENT RESPONSE

A Thesis

by

ZACHARY RYAN LONG

Submitted to the Office of Graduate Studies of
Texas A&M University
in partial fulfillment of the requirements for the degree of

MASTER OF SCIENCE

Approved by:

Chair of Committee,	Mark Everett
Committee Members,	Jean-Louis Briaud
	Hongbin Zhan
Head of Department,	Richard Carlson

August 2005

Major Subject: Geophysics

ABSTRACT

A Near-Surface Geophysical Investigation of the Effects of Measured and Repeated Removal of Overlying Soil on Instrument Response. (August 2005)

Zachary Ryan Long, B.S., University of Louisiana at Lafayette

Chair of Advisory Committee: Dr. Mark Everett

A geophysical survey presents many challenges. A scientist must be able to not only understand the theory and nature of the geophysics being applied but must also be able to identify features of interest in a dataset. It is also of extreme importance to be able to determine where, in the subsurface, the features identified in the data occur.

This research is designed in an attempt to identify the locations of subsurface heterogeneities that affect geophysical instrument response. An experiment was conducted in which topography, magnetics, ground-penetrating radar (GPR), and electromagnetic induction (EM) data were collected over a defined survey line. An excavator with a modified flat-bladed bucket was used to remove, or skim, a 5 to 10 cm thick layer of material from the survey line. Upon removal of the material, datasets from the above mentioned instruments were again collected along the same survey line. This process was repeated for 10 skims, resulting in a total of 11 sets of data for each instrument.

Having collected data with various instruments in the same location as material was progressively removed allowed for an empirical study with the goal of noting how

the response of each instrument changed with respect to the removal of material. By observing how the anomalies changed in the data from one skim to the next, a better understanding of the location of the causative heterogeneities could be had.

Data for each instrument was compared to the equivalent data collected from each subsequent skim to determine how similar or different the data appeared as the depth of the trench increased. The experiment also sought to determine if the topographic variations, or roughness, along the survey line had any impact of the geophysical signals. The data collected from each instrument were compared to the topographic roughness of the survey line for the corresponding skim.

ACKNOWLEDGMENTS

I would like to express my great appreciation to my committee chair, Dr. Mark Everett, for his generosity in offering his time, expertise and willingness to get his hands dirty during the experiment itself. He allowed my experience here to be as enjoyable and beneficial as it could have possibly been. Many thanks are also extended to the other members of my committee: Dr. Jean-Louis Briaud from the department of Civil Engineering and Hongbin Zhan from Geology and Geophysics. Their constructive insights into this project were needed and are greatly appreciated. Additionally I would like to thank all of those who volunteered their time and efforts in taking part in the field portion of this experiment: Carl Pierce, Alfonso Benavides, Doug Sassen, Jamie Collins, and Josh King.

Finally, I would like to thank Aaron Fisher, Bryan Flynn, Tara Kneeshaw and Eric Robinson. Their encouragements and much needed distractions allowed for an unforgettable experience not only at Texas A&M, but in Bryan/College Station as well. Thanks and Gig'em.

TABLE OF CONTENTS

Page

LIST OF FIGURES

Figure Page

Figure Page

INTRODUCTION

The purpose of this experiment and subsequent data analysis is to gain a more thorough understanding of how the signatures of three geophysical instruments are affected by successive removal of known amounts of near-surface sediments. The three types of data collected for this study were magnetics, electromagnetic induction, and ground-penetrating radar. This thesis project was conducted in hopes that the final results would provide geophysicists with a better understanding of the origin and nature of instrument response in near-surface applications. As a result, this would remove a portion of inherent ambiguity of target identification resultant of heterogeneity within the geologic environment.

The primary question addressed by this research was: *Where, in the subsurface, do geophysical signal anomalies originate?* That is to say, is it possible to discern a correlation between the material being removed and the signatures of each of the instruments used for this experiment? With appropriate analysis techniques of data acquired over the same track following repeated soil skims (10 skims, or soil removal operations, were conducted with this experiment), it was hypothesized that patterns or trends would be revealed. It was also hypothesized that the data from soil skims close to one another (small skim lag) would correlate well with the degree of correlation decreasing as the data are compared to those of later skims (large skim lag). For

---

This thesis follows the style of Journal of Applied Geophysics.

example, data collected after skim 1 was expected to be more similar to data collected after skim 2 rather than skim 10. Figure 1 shows this using R-squared, a statistical measure of the suitability of data to a trend, plotted against skim lag, or the proximity of the skims being compared. As the lag of compared skims increases, it is expected that the correlation value will decrease at some rate.

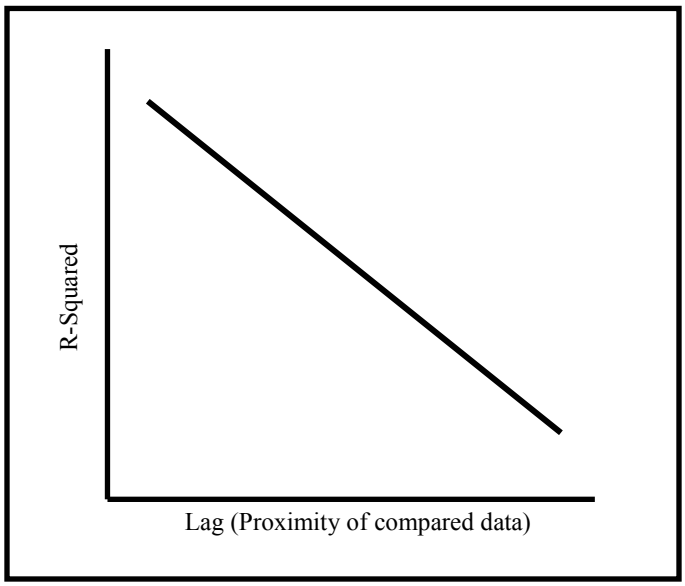

Figure 1. Hypothesis of data correlation with respect to lag.

Geophysical surveys produce two inherent challenges. First, one must be able to identify targets or features in interest in a dataset. Secondly, after the target has been identified, it is imperative to be able to translate the location of the target in the dataset to a specific point in the subsurface. This survey seeks to understand the nature of

geophysical signals with depth by observing changes as they become earlier in the time section as a result of the soil skims and their disappearance when the causative heterogeneities are removed with a skim. Positive results from this research would serve to aid development of current and new geophysical techniques for studying the human-impacted environment, including archaeology and the detection and discrimination of landmines and unexploded ordnance (UXO) by allowing for a better understanding of where in the subsurface the target responses are being generated. The proliferation of the latter is a consistently increasing problems on a global scale (Zoubir and Chant, 2002). The results could also have implications relevant to geophysical prospecting for various engineering efforts, such as tunnel detection and utility inspection, and geological applications, such as fault detection and stratigraphic mapping.

BACKGROUND STUDIES AND PREVIOUS WORKS

When this experiment was designed, it was understood that this was an innovative project. Upon further investigation it was discovered that little other similar research has been conducted for this purpose. Numerous academic and military groups, including Nyquist et al (2005), have sought to determine how geologic and other noise interact with the target signal of various geophysical instruments. Archaeologists have done similar studies using GPR to locate and characterize buried objects throughout excavation processes, however, both the scale and precision of their efforts are markedly different from this research (Malliol et al, 2005). With respect to EM induction, Benavides and Everett (2005) and Everett and Weiss (2002) have conducted studies concerning effects of geologic noise and buried conductive targets on the received signal. Similarly, Butler (2003) has used the contrasts between magnetic backgrounds of various soils and UXO properties in an investigation to determine detection probabilities in different conditions. The above studies all have similarities to this research in that they attempt to gain a better understanding of how the near-surface geology affects instrument response. This study differs, however, in that it utilizes the progressive removal of soil in an attempt to determine the location of the subsurface heterogeneities that produce the background signal in a dataset.

INSTRUMENT DESCRIPTION AND THEORY

Magnetics

Global-scale magnetics was one of the first areas of geophysics to be studied and localized magnetic anomalies were being investigated as early as the mid 1600's (Sharma, 1997). Since then, magnetic surveys have proven to be extremely valuable in the study of both small-scale objects that are relevant to engineering, archaeology and environmental science as well as larger scale anomalies that give information of regional geologic structure (Lillie, 1999). It is an extremely cost-effective and time-efficient method relative to other geophysical surveys. Magnetics data are often used in conjunction with other data sets, such as gravity, to support to geological interpretations (Milligan and Reed, 2004).

A geophysical magnetics survey is a passive technique in that the instrument is not actively magnetizing the soil but rather simply measuring the earth's ambient magnetic field. The signal recorded by the instrument in a magnetic survey is produced by variations of the magnetic properties of the subsurface rock or soil. The primary factor governing the magnetic response of a soil is the relative abundance of magnetic minerals (Sharma, 1997). In order to quantify the ability of a particular material to become magnetized in the geomagnetic field, a dimensionless value, known as the *magnetic susceptibility*, is assigned (Gattacceca et al., 2004). Highly magnetic minerals, such as magnetite and maghemite, have magnetic susceptibility values on the order of 0.1. Conversely, less susceptible materials like granite and sandstone have values of

.00001 and .0001, respectively (Lillie, 1999). The signal generated by a magnetometer will change accordingly with variations the abundance, distribution and magnetic susceptibility of materials in the subsurface. Non-natural target objects, such as UXO and buried iron (i.e. rebar within reinforced concrete foundations or pavement) have susceptibilities on the order of 100-500 which are significantly higher values than those of the most susceptible natural minerals.

For this experiment a Geometrics G-858 Cesium-vapor magnetometer in vertical gradiometer mode with top and bottom sensors will be used (Figure 2). This instrument measures the magnetic field by noting variations in energy resultant of the internal electrons changing orientation in response to an applied radio frequency (RF) field superimposed on the external geomagnetic field. This energy difference is equal to the product of the strength of the geomagnetic field times an atomic constant (Smith, 1997).

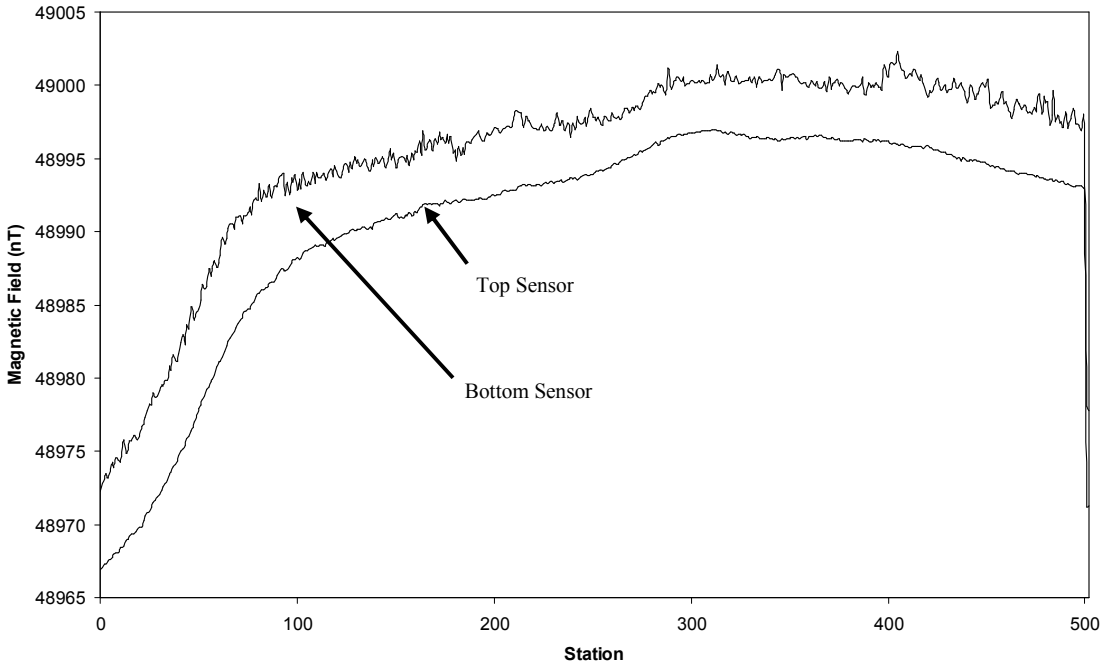

Figure 2. Example of raw magnetics data showing top and bottom sensor data.

The Cs atom has one electron orbiting freely in the outermost shell. Because this electron has a charge and spin, it also has a small magnetic moment and is, therefore, influenced by the presence of a magnetic field. The electron energy levels exhibit a Zeeman splitting as the spin interacts with the applied magnetic field.. Noting the magnitude of the Zeeman effect allows for the determination of the external magnetic field (Smith, 1997).

This particular instrument was chosen for multiple reasons. Firstly, the alkali-vapor magnetometers are capable of detecting variations in the ambient magnetic field that are on the order of .01 nT. To help quantify the sensitivity of this instrument, the average intensity of the Earth's magnetic field is around 45,000 nT, varying from 30,000

nT at the equator to 60,000 nT at the poles (Sharma, 1997). Natural soil variations, however, generally exhibit changes on the order of 50 nT (Dalan and Bevan, 2002). The use of a sensitive magnetometer will allow for a detailed analysis of extremely small magnetic anomalies along the survey line. Another reason for the selection of this instrument is that it has a higher sampling rate than other types of magnetometers and orientation of the instrument during a measurement is insignificant, making data acquisition time efficient (Sharma, 1997). Additionally, a Cesium-vapor magnetometer can be operated by a single person as it requires only one touch of a button to record a measurement.

Ground Penetrating Radar (GPR)

Over the past few decades, the GPR method has been employed in near surface investigations to locate numerous targets of a diverse nature. From faults to pipes and groundwater to targets of archaeological interest, GPR has proven to be an efficient and reliable survey method (Davis and Annan, 1989). It is because of the exciting potential and increasingly important role of GPR in geophysics that it has been selected for this project. Results obtained from the GPR in a successful skimming experiment would have implications for many areas of geophysics.

The GPR method uses the transmission of high-frequency (25-900 MHz) electromagnetic waves into the subsurface to determine the locations of impedance discontinuities by measuring the time, location, and amount of energy reflected to the

surface (Sharma, 1997). Here, discontinuities are represented by changes in the square root of the product of the relative dielectric permittivity (RDP) and magnetic susceptibility of subsurface materials (Zoubir and Chant, 2002). RDP is a measure of the ability of a material within an electromagnetic field to become polarized (Bano, 2004). The dielectric constant of a material can vary significantly over a survey area as it is influenced by the texture of the subsurface material as well as the water content (Hendrickx et al., 2003). Models have also been developed that use soil texture and water content to predict dielectric constants and these have proven to be consistent with measured values (Dobson et al., 1985). Figure 3 shows a cross-section view of the travel paths of an EM wave generated by a GPR transmitter in a two-layer scenario, with Layer 2 having a greater RDP value than Layer 1.

A GPR instrument is comprised of two antennae, one to transmit the electromagnetic pulse and the other to receive the signal returned from the subsurface reflectors (Figure 3). The antennae are connected to a central console that controls the firing of the transmitter and stores the data acquired by the receiving antenna. The console is, in turn, linked to a laptop computer where the operator is able to trigger data acquisition as well as view the signals received while a survey is in progress. A GPR data set looks very similar to a seismic time section in that it is composed of individual wiggle traces that exhibit different amplitudes and polarities based discontinuities within the subsurface (Sun and Young, 1995).

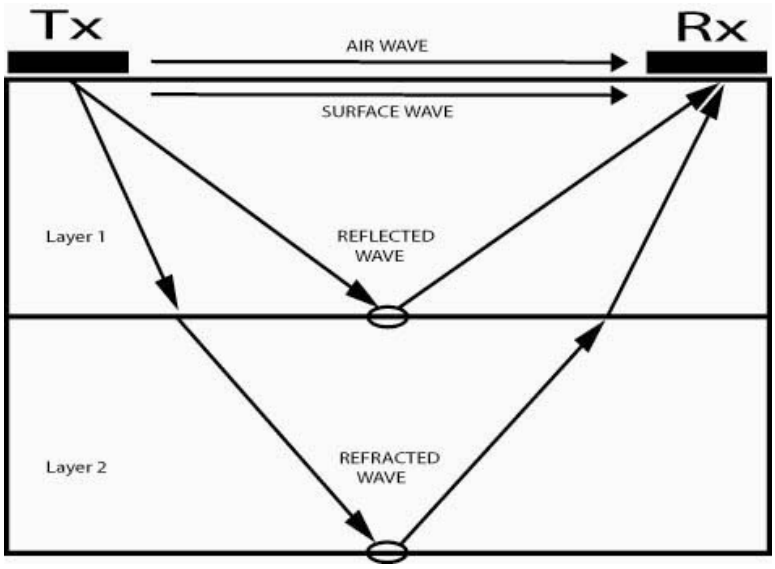

Figure 3. GPR wave paths from transmitter (Tx) to receiver (Rx).

The GPR unit chosen for this experiment is the Sensors & Software Pulse_EKKO 100 with 200 MHz antennae. The antenna frequency was chosen based on the penetration depth and resolution needs of the experiment (Van Dam and Schlager, 2000). The vertical resolution of GPR antennae is practically defined as the half-wavelength of the wave in a geologic medium. Using an assumed EM wave velocity of 10^8 m/s and a center antennae frequency of 200 MHz, a vertical resolution of roughly 30 cm is expected (Basson, 1992) As this survey deals with detailed signal analysis of the upper few meters of soil, high resolution is of more importance than greater depth of penetration, thus the highest possible frequency antennae for the Pulse_EKKO 100 were chosen.

Electromagnetic Induction (EM)

Electromagnetic induction was first discovered by experimenters in the early 1800's. Modern geophysical electromagnetic induction techniques have been researched and applied for decades (Atherton, 1980). A prominent and applicable product of this science is a landmine detector. The military has been using detectors for decades in war zone remediation and they have proven to be invaluable tools. Recently, however, the conventional metal detector is no longer an effective means of mine identification as most modern mines are constructed primarily of synthetic materials with little or no metal present (Zoubir and Chant, 2002). The importance of EM induction to the military has not subsided due to the increasing research being done in the field of UXO detection and discrimination.

The Geonics EM-63 employs a transmitter/receiver configuration that is conventionally used in a cart-mounted fashion.

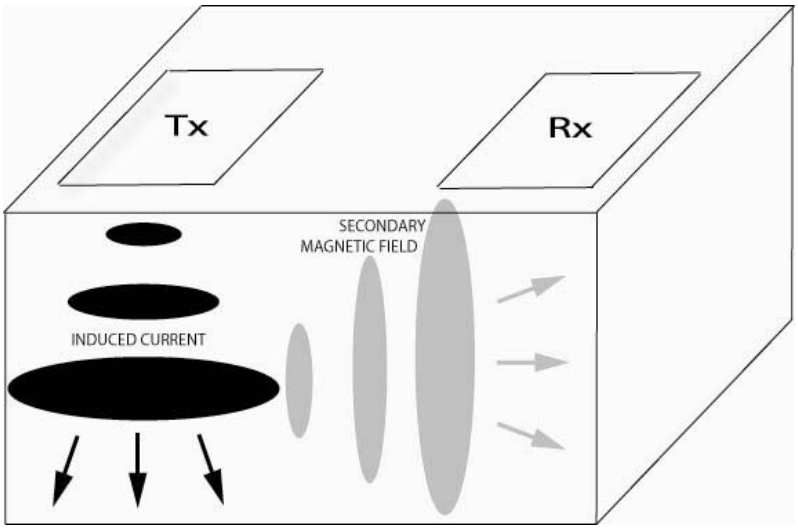

Figure 4. Basic EM instrument transmitter (Tx) and receiver (Rx) configuration and wave propagation.

For this study, however, the receiver coil will be placed inside the transmitter loop, creating what can be viewed as a zero-offset survey that will provide better data resolution as the receiver coil will be closer to the source of the secondary magnetic field. Figure 4 shows an offset Tx/Rx configuration to allow for a clearer illustration of the basic EM induction physics, which is based on diffusion of EM fields. A steady current is established in the transmitter and is sustained for a sufficient period such that resultant transient eddy currents in the ground are allowed to dissipate (McNeill, 1980a). When a measurement is ready to be taken, the current is abruptly shut off establishes an electromotive force (emf) in nearby conductors (Sharma, 1997). The emf produces a secondary magnetic field whose intensity is related to the emf and, thus, decays in a proportional manner. The rate of decay is diagnostic of the conductivity, size and shape

of the conductor. The secondary magnetic field is measured by the receiver coil at logarithmically spaced time intervals (McNeill, 1980b). The electrical conductivity of the material in the subsurface has a strong influence on the nature of the EM diffusion. Soil electrical conductivity is a measure of how charge carriers migrate through the bulk material and is influenced by such factors as mineralogy, soil aggregation, and soil water (Hartsock et al, 2000). In general, clays are much more highly conductive than sands with conductivity increasing as soil water is introduced and further as the salinity of the water increases (Sharma, 1997).

EXPERIMENT SITE CHARACTERIZATION

The Texas A&M University Riverside campus was chosen as the location to conduct the field portion of the skimming experiment. This site was initially thought to be composed primarily of overflow and other floodplain sediments from the Brazos River. A post-experiment inquiry, however, revealed that the site was previously used to train earth excavator operators. The repeated excavation activities effectively homogenized the site by erasing the natural geologic heterogeneities. This likely had a profound impact on the physical properties of the soil (Dalan and Bevan, 2002). Though these findings did not alter the validity of the experiment, the nature of the site was poorly suited for this particular project as it was ultimately too homogenized to produce the strong, consistent background signals desired. In addition, it was not possible to study natural geologic variability.

Soil samples collected during the experiment were examined to identify changes in mineralogy, saturation content and other physical properties that may be present along the length and depth of the survey area. Preliminary results, however, showed that the soil was quite homogeneous throughout the experiment. The saturation analysis, done using soil collected at the 10 m and 40 m locations of the survey line for each skim, showed variations of 8.89% in water content, ranging from 13.2% to 21.09% with an average value of 17%. Additionally, these moisture variations, though small, occurred in no discernable pattern with respect to location along the survey line or depth of the trench. These results are positive in that the differences in soil moisture are not

substantial enough to have a significant variable impact on the data. An x-ray diffraction analysis was performed on the samples to better understand the mineralogy of the soil. The results very closely matched the Burleson and Ustarents soils units described in the 2002 *Soil Survey of Brazos County, Texas,* which can be found at *http://soils.usda.gov/survey/online_survey/texas*. The two soil types are nearly the same, with the exception being the Ustarent unit having been disturbed due to gravel mining. The Burleson clay seems to fit the experiment site more closely, however, as a change in soil color was noted at the depth at which it is described in the soil survey at about 1.2 m. Diffraction results for this unit show that the constituent clay particles (<0.002 mm) were composed of hematite, kaolinite, mica and montmorillonite.

EXPERIMENT PARAMETERS AND PROCEDURES

The first step in the project was to clearly define a 50 m transect over which profiles were to be run with the GPR, magnetometer, and EM-63. This was done by placing survey stakes at the 0 and 50 m points along the transect. Subsequently, stakes were placed at the 10 and 40 m locations which served as the outer boundaries of the 30 m section to be skimmed, allowing the first and last 10 m sections of the transect to remain undisturbed throughout the experiment. The width of the trench region was roughly 5 m and was sufficient to render negligible any influence the walls may have on the instrument's responses. A flexible field tape was fastened to the endpoints of the survey line and allowed measurements to be taken at consistent predetermined intervals with each instrument. The final step in site preparation was to walk the survey line with a Schonstedt magnetometer, a ferrous metal detector, and remove any such items found in order to minimize the potential for data influence from non-natural sources. Once the survey area had been marked and cleaned, the setup process was complete allowing for the start of data acquisition. Figure 5 shows a plan view of the survey area.

The first profile with each of the three instruments was acquired over the undisturbed soil in order to obtain a background data set. Due to technical complications with the GPR unit, a background radar dataset was not collected. In addition to the geophysical instruments, a total station survey instrument was employed to collect microtopography values along the transect relative to the base station (0 m) location at .5 m intervals for a total of 101 measurements per skim. This information was necessary as

it was used in subsequent analyses to determine whether the signal of each of the instruments was influenced by the topographic variations of the profile.

The first survey was done with the magnetometer. Upon assurance that the surveyor had no magnetic material on his person, the data collection began at the 0 m point on the survey line. From there, a magnetic reading was taken every .1 m for a total of 501 data points per 50 m profile. At the completion of the magnetics survey, the EM-63 was positioned over the 0 m point and prepared for data collection. The sled-mounted system was pulled at .5 m increments for the length of the survey line, which resulted in 201 total measurements for each transect.

The GPR survey was done last with data collected every .25 m over the length of the survey line. As previously mentioned, an initial dataset was not collected due to instrument complications which are discussed in more detail in the *GPR Analysis* section. For the purpose of subsequent lab analysis, soil samples were collected at 5 m intervals over the trench portion of the survey line (10 m to 40 m) and stored in air-tight containers to preserve the in situ moisture. Examination of the collected samples was intended to be used as an aid in the understanding of how the responses of each instruments are expected to change due to variations in soil properties. These samples were not used in this research as preliminary analyses of the samples exhibited very little variation throughout the length of the trench. These results were likely resultant of the soil homogenization caused by human activities.

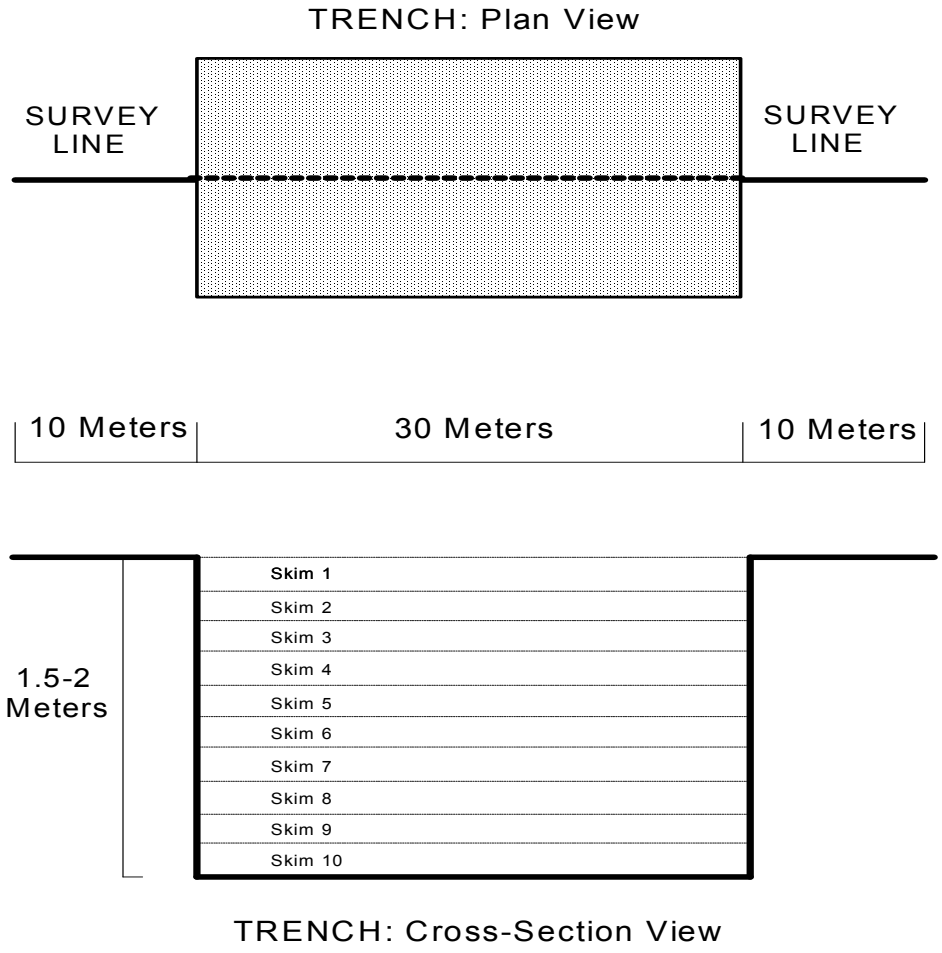

Figure 5. Experiment site layout.

Upon completion of the above processes, the experiment was ready for the removal of the first layer of soil (the first skim). To accomplish this for each skim, a bucket excavator was employed. In order to achieve a smooth surface as material was removed, a flat-blade was welded to the teeth of the excavator bucket. As the length and width of the trench area had been outlined with survey paint at the time of setup. The material within those boundaries was removed to a depth of .15-.2 m. The excavation process was done as precisely as possible given the time constraints of this experiment. Archaeologists, for example, use very time-consuming methods to achieve accurate and uniform skims. This experiment required a balance between precision and efficiency. Knowing that there would be significant variability in the soil removal, the total station was used to reveal exactly how much material was excavated at each measurement point after each skim. The excavator was positioned 2-4 m off of the survey line and moved parallel to it as the flat-blade welded to the bucket skimmed the soil in a direction perpendicular to the line of travel. When the first layer of material was removed over the length of the trench, the machine was moved away from the survey area so as not to interfere with the geophysical instrument responses.

Having completed the first skim, the total station was employed to collect the microtopography information. The magnetics and EM surveys were then carried out at the same sampling intervals that were used to collect the background data. By this time, the GPR problems had been remedied and data were collected at .5 m intervals. Finally, soil samples were again collected, labeled and stored for analysis at a later time. After skim 2, because rapid progress was being made, the station interval for EM data

acquisition was decreased to .25 m which provided better data resolution over the survey area. For the same reasons, the GPR station interval was changed to .25 m after skim 1.

The above procedures and processes were carried out for ten skims, which yielded a final trench depth of roughly 1.7 m. The data collected before any material was removed are referred to as skim 0 data, with each other dataset corresponding to the skim number from which it was collected. The number of skims and final trench depth provided a sufficient amount of data and sediment removal respectively to carry out an effective signal analysis for each of the instruments used.

DESCRIPTION OF STATISTICS USED

In the data analysis phase of this research, numerous scatter plots were made in order to display any trends that were present. While much could be learned from a visual assessment of the results, it is important to quantify the relationships to determine how trends vary from one dataset to the next. Two primary statistical procedures were employed to serve as standard analyses.

Linear Regression

Linear regressions were used heavily throughout this research to describe trends in the data. In a most basic description, a linear regression is a calculation that applies a best-fit line to a series of data points. The benefit of this procedure is that it provides an equation of the form

$$y = a + bx$$

where a is the value at which the best-fit line crosses the y-axis, b is the slope of the line and x and y are the coordinates of any point on the chart. The linear regression, thus, provides a straight line that most accurately describes the distribution of the data. The best-fit line can be used to predict the value of one variable, either x or y, if the other is known.

A linear regression can be performed using most graphing software with the simple click of a button. It is important, however, to understand how the computer is obtaining the results displayed on the chart. A linear regression is found by using the *least squares regression* equation which is

$$y = -\frac{\hat{a}}{\hat{b}} + \frac{1}{\hat{b}}x$$

where $\hat{a}$ and $\hat{b}$ are the least square estimates of a and b. The values of $\hat{a}$ and $\hat{b}$ are found using the following equations in which *N* represents the number of data points present in the analysis.

$$\hat{a} = \frac{\sum_{i=1}^{N} y_i}{N} - \hat{b}\frac{\sum_{i=1}^{N} x_i}{N} = \bar{y} - \hat{b}\bar{x}$$

$$\hat{b} = \frac{\sum_{i=1}^{N} x_i y_i - \frac{\sum_{i=1}^{N} x_i \sum_{i=1}^{N} y_i}{N}}{\sum_{i=1}^{N} x_i^2 - \frac{\left(\sum_{i=1}^{N} x_i\right)^2}{N}}$$

The goal of these equations is to minimize the sum of the squares of the distances between the data points and the straight line produced by the regression. If there is a strong trend in the data, the linear regression will provide a very accurate representation of the data. If the data occur in a random distribution, a regression can still be calculated but will have very little significance in describing the behavior of the data.

R-Squared

When calculating a linear regression, it is important to note the suitability of the line with respect to the data point distribution. As previously mentioned, a regression can be calculated for data that exhibit no apparent linear trend and, in that situation, the resultant line cannot be regarded as scientifically meaningful. Calculating R^2 values allow for a numerical description of the degree by which the data support a regression. R^2 values range from 0, meaning there is no relationship between the data and the regression, to 1, in which case all data points fall directly on the regression line. In other words, it describes the percentage of data points in agreement with the regression or the

relative predictive power of the regression. For example, an R^2 of .653 indicates that typically 65.3% of the data points would obey the trend characterized by the linear regression. As with the regression, R^2 can be immediately found using graphing software. The equation used, however, is

$$R^2(x,y) = \left[\frac{\mathrm{cov}(x,y)}{StdDev(x) * SdtDev(y)} \right]^2$$

where *cov,* the covariance, is the statistical measure of correlation of the fluctuations of two different quantities. Similarly, the standard deviation, *StdDev*, is the measure of the distance a quantity is likely to lie from the mean value.

MAGNETICS

Introduction

The magnetics data were acquired in a very efficient and consistent manner as the instrument is designed such that measurements can be taken very quickly. The station separation was held constant for each of the eleven datasets collected. It was determined that, because of the speed with which a magnetic profile could be made, the distance between measurements would be .1 m, resulting in a total of 501 data points along the 50 m survey line. Upon completing preparation of the experiment site, the Geometrics GS-858 cesium-vapor magnetometer was assembled. After ensuring the operator was clean of any items that might influence the surrounding magnetic field and allowing a ten-minute period for the instrument to warm up, the first dataset was ready to be collected. Beginning at the 0 m indicator on the measuring tape, the first measurement was recorded and was followed by acquisition at each .1 m mark thereafter, ending at the 50 m point. This process was carried out in the same manner for each of the ten subsequent profiles, each representing a different skim.

The magnetics component of the experiment was successful in that data were collected after each skim as well as the pre-skim background, with all profiles having the same number of data points. A problem did arise while in the process of collecting data after the third skim. The operator noticed that the instrument had begun to function improperly, as the readings produced were incongruent with those recorded earlier in the experiment. The skim 3 dataset is shown in figure 6, highlighting the problem area. A quick inspection of the magnetometer revealed a loose connection between the console and batteries. The problem was quickly remedied and the remainder of the survey was completed.

Preliminary Data Correction

As a result of the improper battery connection several data points recorded were not valid and needed to be corrected prior to any analysis of those data. In the skim 3 dataset the bottom sensor produced problematic values for sixteen consecutive stations, representing 1.6 m along the survey line, while the top sensor was not working properly for the last six of those stations.

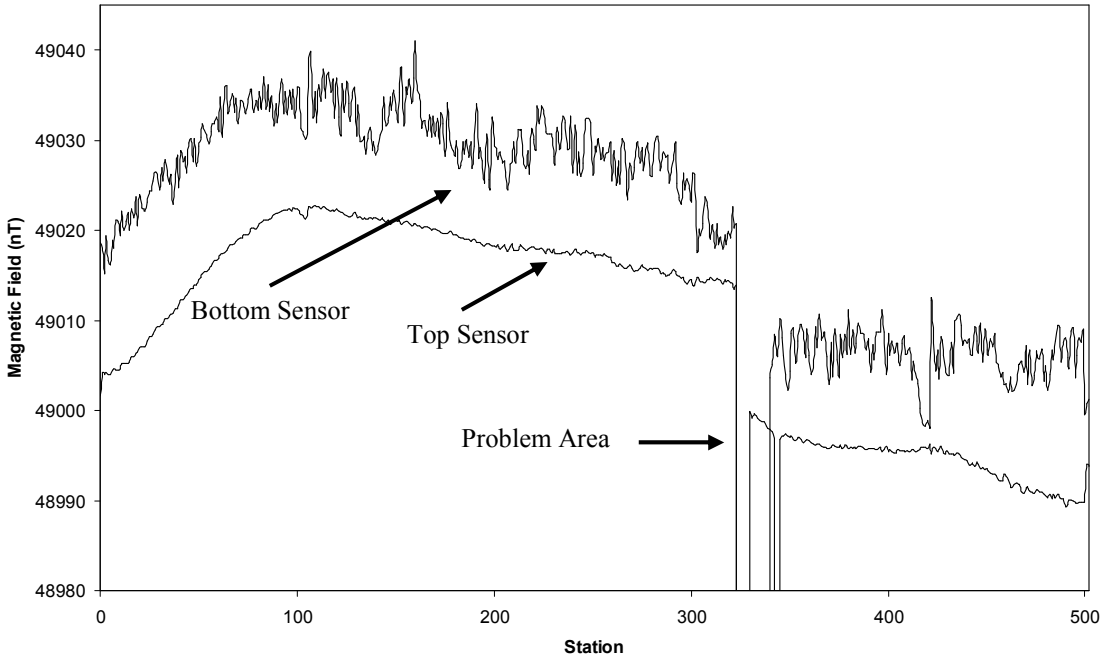

Figure 6. Skim 3 magnetics data showing problems resultant of improper battery connection.

Because of the large number of stations, it was possible to interpolate the unknown values with an acceptable level of accuracy. Corrections were made to the top sensor first. The last correct value before the instrument malfunctioned was located at station 323 and the first value recorded after the problem was solved was found at station 330. The difference of these two measurements was taken and then divided by their spatial separation, which was six stations. The resultant value was added to the recorded value at station 323 to produce the interpolated measurement for station 324. This process was iterated for stations 325 through 329, in each case adding the calculated average change to that of the previous station, resulting in a linear increase in values from station 323 to

330. This method was acceptable for the top sensor because the error occurred over very few stations. The problem with the bottom sensor values, however, necessitated a different course of action. Because the values of the two sensors subtly mimic one another, an average of the difference of the measurements between the top and bottom sensors for each station was calculated. That average was then added to the top sensors values to produce corresponding absent bottom sensor value. The result was a bottom sensor curve that mirrored that of the top sensor simply at a higher set of values. This correction process, though not an exact substitute for measured values, produced results that were satisfactory in that the corrected points then had a much less errant influence on the subsequent analyses (Figure 7).

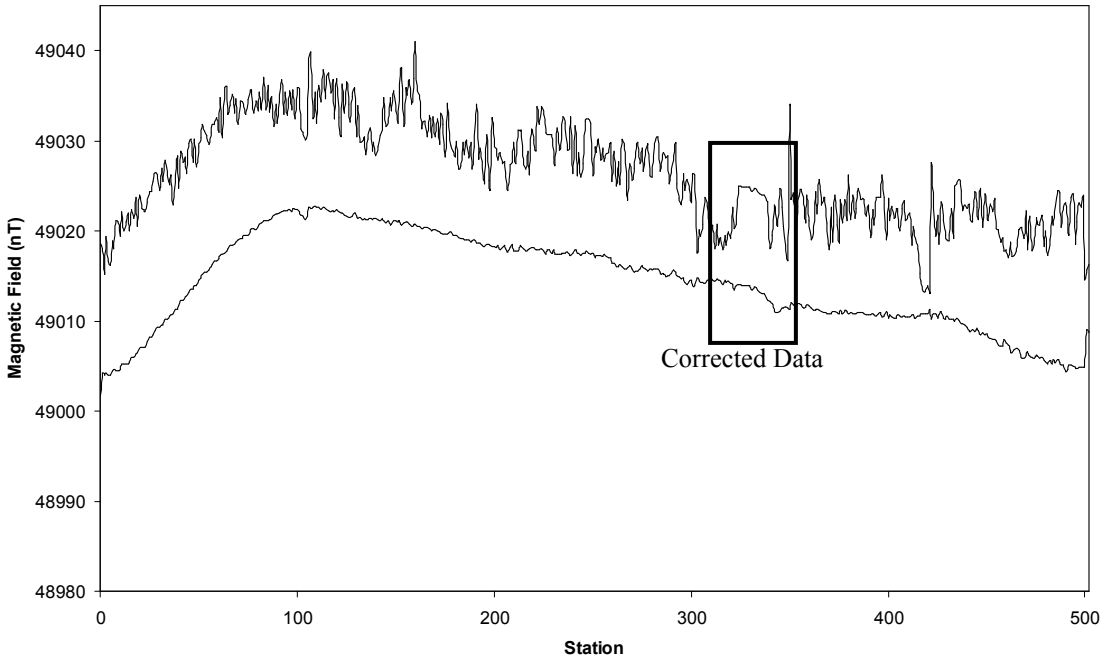

Figure 7. Skim 3 data corrected for improper battery connection.

Magnetic Roughness

The first study conducted using the magnetics data sought to determine if a relationship existed between the data and topography values over which those data were collected. To do this, the roughness of both the magnetic and topographic signatures needed to be calculated and this was done for each using the following formula where f_i is the value of the data at station i and N is the total number of stations.

$$R(f) = \frac{1}{n}\sum_{i=1}^{n-1}\left|f_{i+1} - f_i\right|$$

For each skim, the absolute value of the numeric difference between each of the 501 stations was calculated, resulting in a new set of 500 numbers. The average of those numbers was found leaving one number for each skim representing the average amount of signal change between stations for that particular skim. Those roughness values were then plotted (Figure 8) in order to obtain a visual assessment of how the signal variance of the skims related to one another.

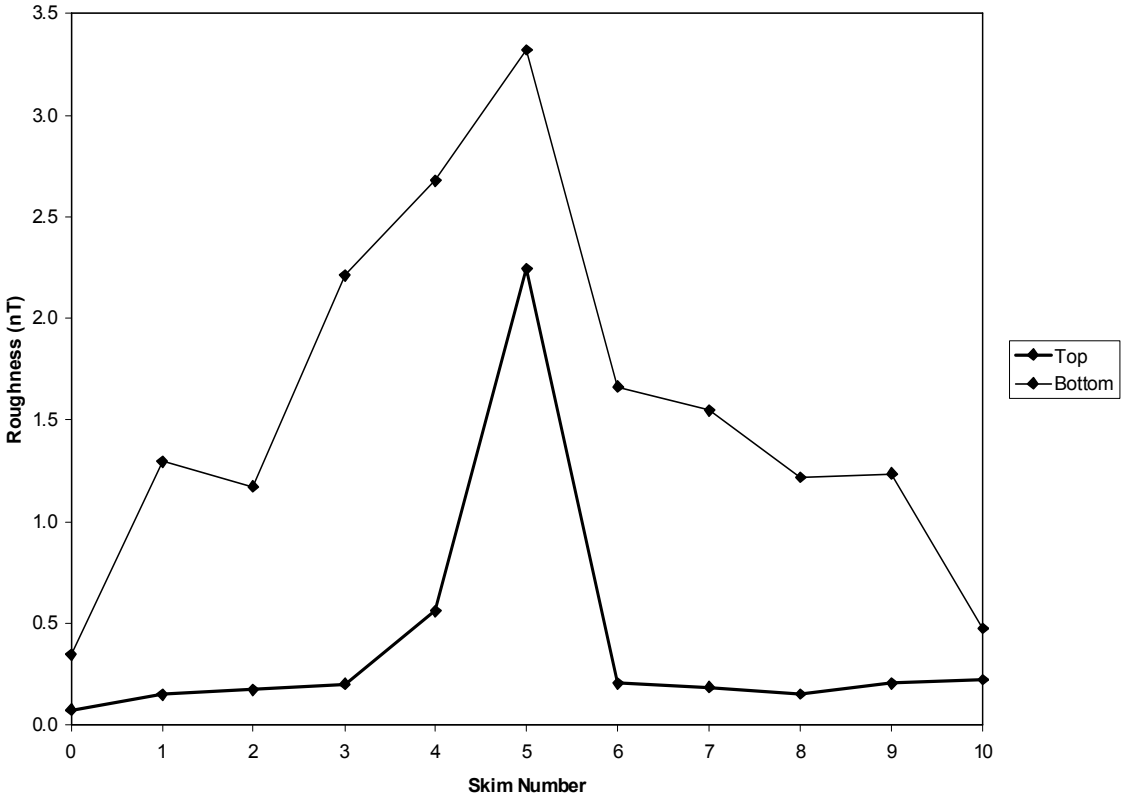

Figure 8. Magnetic roughness for each skim from top and bottom sensor data.

Because the goal of this analysis was to attempt to correlate magnetic signal variations to those of topography, the roughness of the topographic data was calculated and plotted in the same manner as shown in Figure 9. As a result of these operations, there were eleven magnetic roughness values and eleven topographic roughness values, one for each respective skim. The two sets of numbers were plotted against one another with the y-axis representing the magnetic roughness and the x-axis representing the topographic roughness.

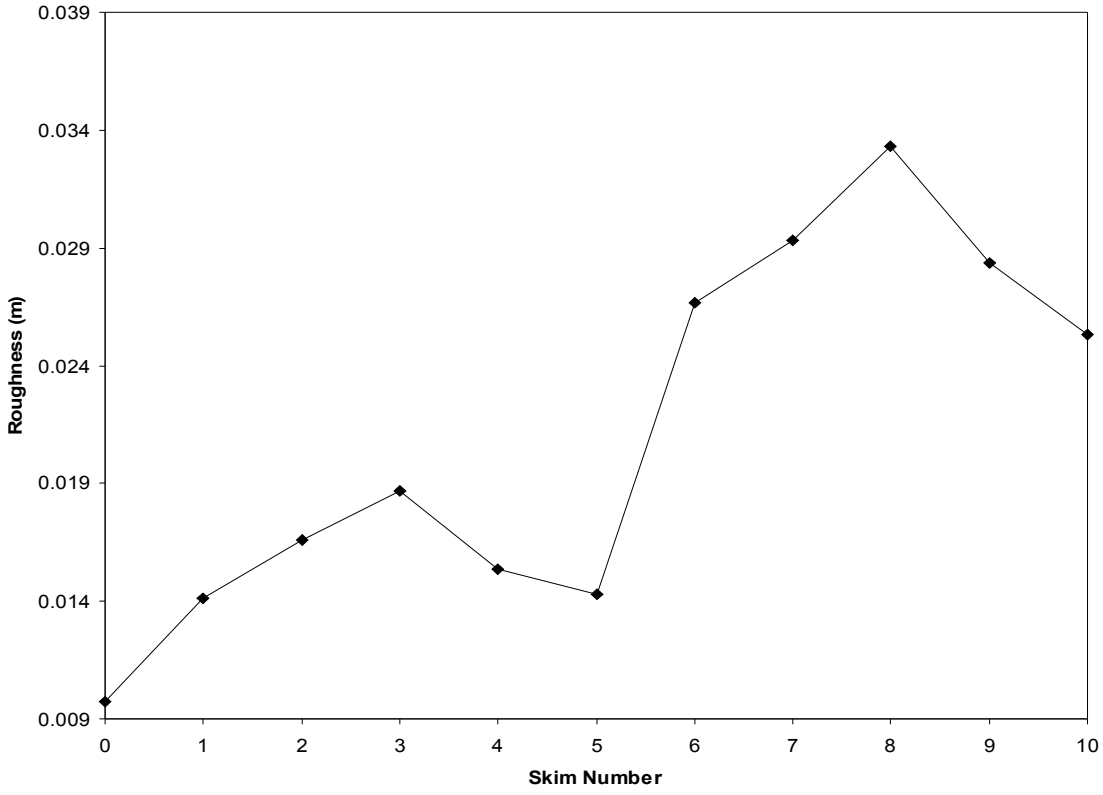

Figure 9. Topographic roughness for each skim.

Magnetic Roughness Results

If a relationship existed, the data points on the scatter plot would reveal the trend. Consistently increasing points would suggest that as the topography becomes more variable, the magnetic signature, independent of physical subsurface variations, would also become more rough. Conversely, a decreasing trend in the point distribution would

imply a rougher survey area generates a muting effect on the magnetic data. The result, however, was in compliance with neither trend. The points occurred in a random distribution, showing that the variations in microtopography throughout the survey area had no systematic effect on the magnetic data (Figure 10). These results were seen as positive as they indicated that no additional corrections needed to be made to the data and that the data were influenced solely by subsurface magnetization variations and not topographic conditions.

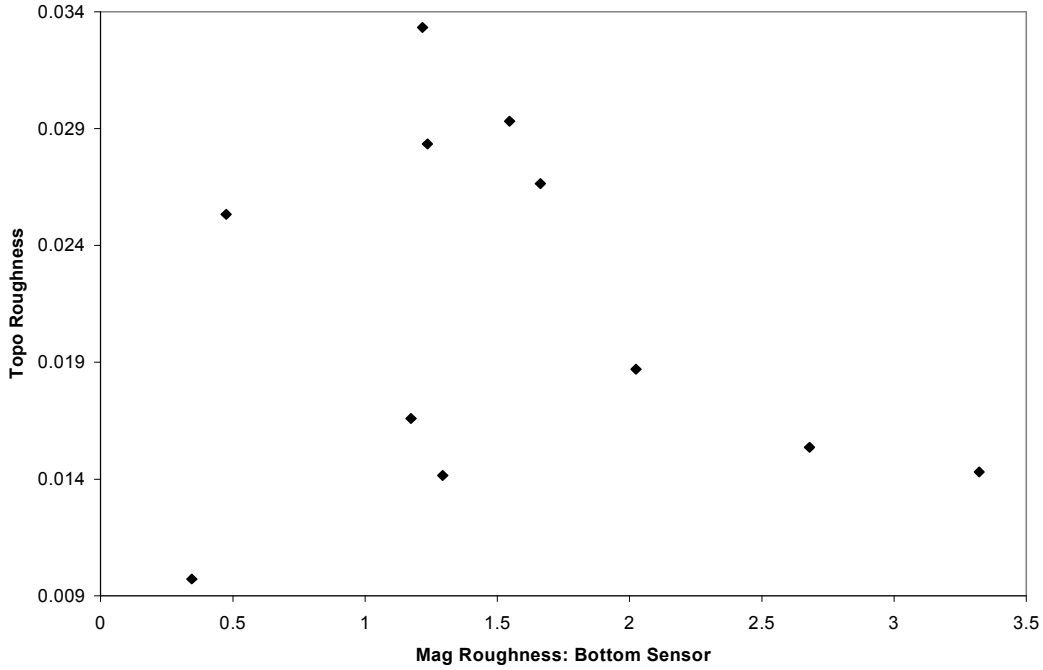

Figure 10. Topography roughness vs. magnetic roughness.

Amplitude Analysis: Bottom Sensor

The second operation performed on the magnetics data attempted to show how the signal changes at a given station as a function of skim number. The data compared were composed only of those stations within the interior 20 m of the trench, or meter marks 15 to 35 along the survey line, so as to examine only the area of consistent soil removal and not the trench ramps or the un-skimmed portions on either side of the trench. The first step involved eliminating all extraneous data to this analysis, leaving top and bottom sensor data from stations 150 to 350 for each skim (Figure 11).

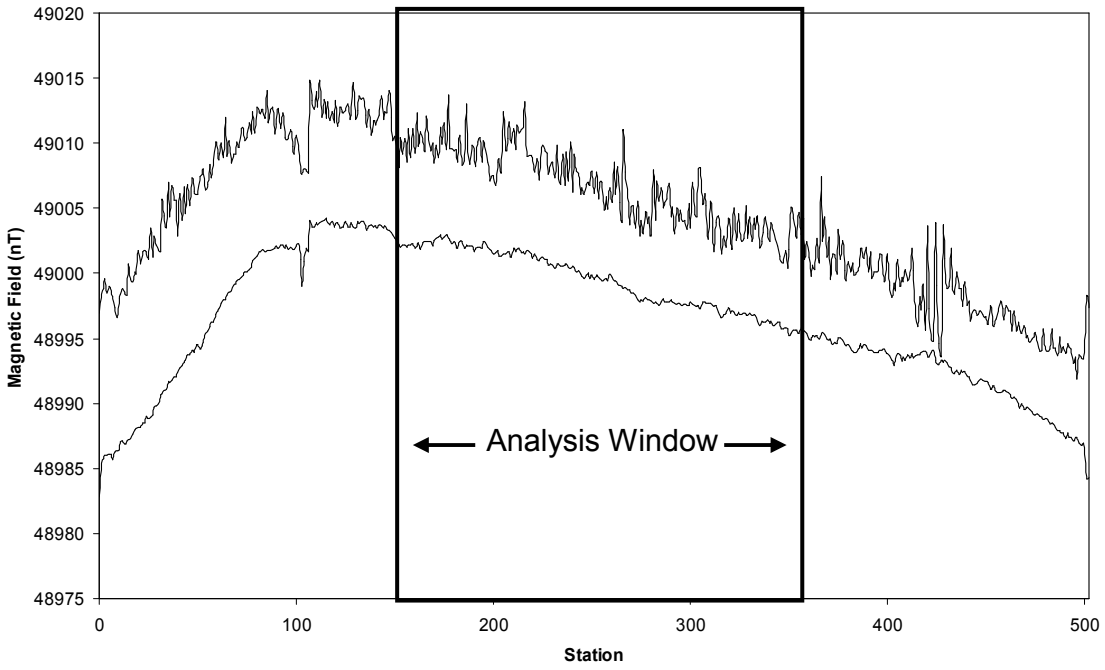

Figure 11. Example of portion of magnetics data for each skim included in the analysis.

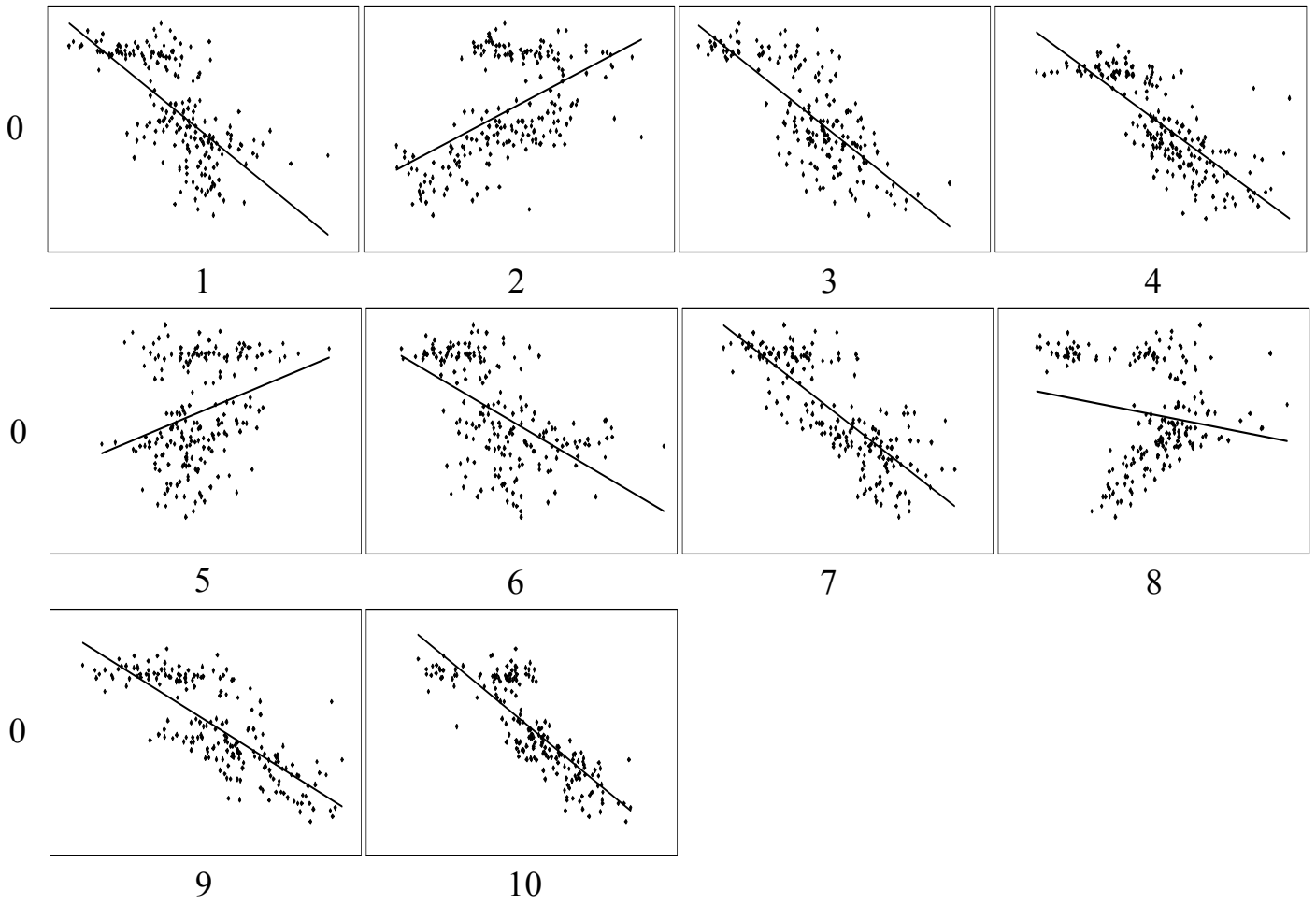

Figure 12. Example of bottom sensor amplitude analysis results as skim 0 magnetics data are plotted against the equivalent data from skims 1 through 10.

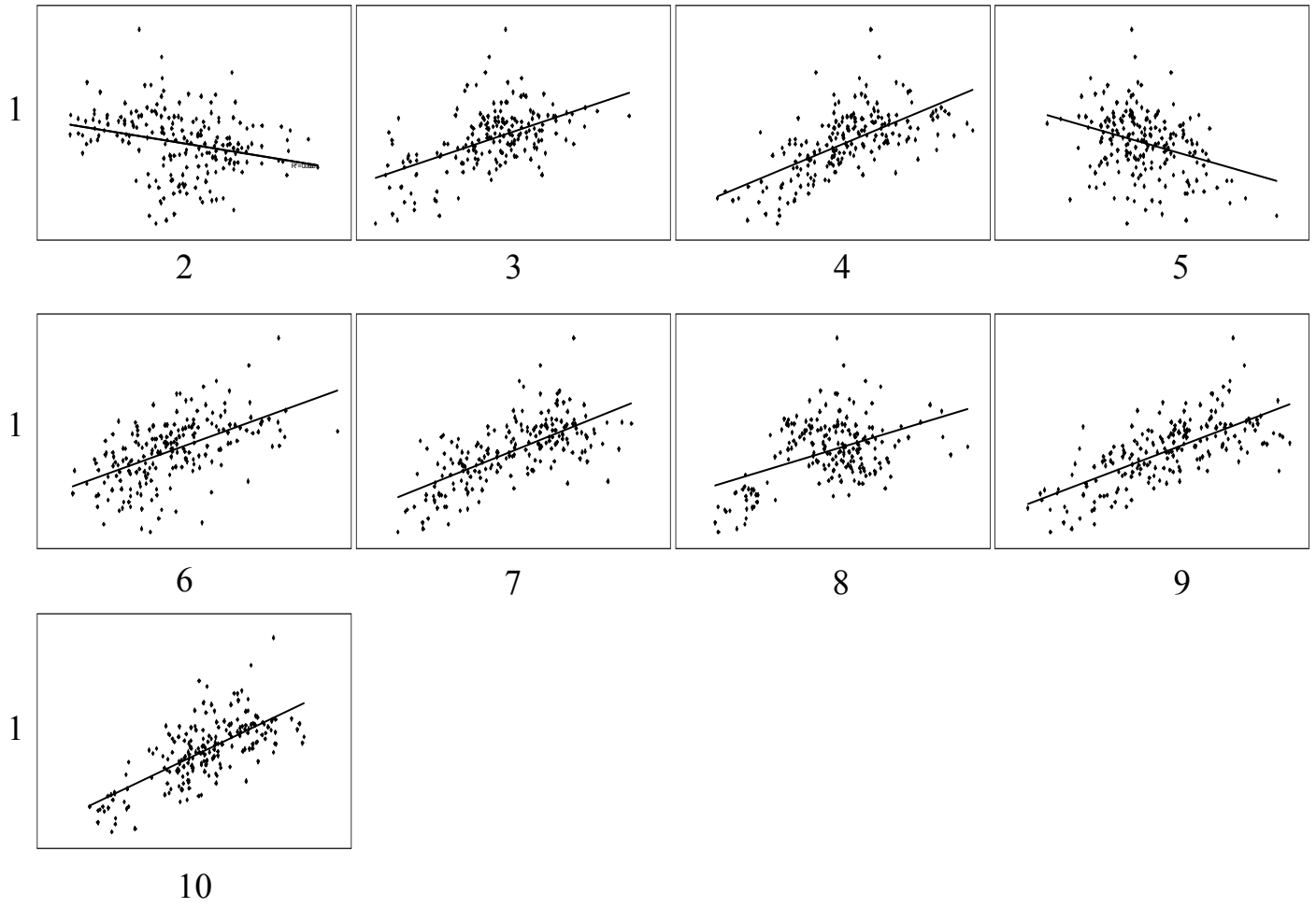

Figure 13. Example of bottom sensor amplitude analysis results for skim 1 magnetics data are plotted against the equivalent data from each subsequent skim.

The process began with the data collected from the background survey, or skim 0. The skim 0 bottom sensor values were plotted as the y-data and the equivalent information from skim 1 was plotted as the x-data. Similarly, the skim 0 data were plotted against the bottom sensor values for each of the other skims resulting in ten scatter plots that displayed the relationship between the relevant skims. The same operation was performed using skims 1 through 9 as Y-values plotted against each subsequent skim for a total of fifty-five comparisons and examples are shown in Figures 12 and 13. To obtain a numerical characterization of the strength of the trends in each plot, a linear regression was made and the R^2 values were calculated (Figure 14). The linear regression provided both the slope and the polarity, either positive or negative, of the correlation while the R^2 numbers served as indicators of the strength of the trends.

Amplitude Analysis: Bottom Sensor Results

As mentioned in the introduction, it was expected that the comparative plots would exhibit a positive, linear relationship or an upward sloping trend with the strength of the correlation dissipating as the differential or lag between the skims increased.

The bottom sensor magnetics data, however, do not support this hypothesis. Each skim 0 comparison with other skims shows mild trends of both direct and inverse nature with the strongest correlations generally occurring at larger skim lags, the opposite of what was expected. The inconsistency in polarity of the trend was also unexpected. Only skims 2, 5 and 8 showed a positive trend when compared with skim 0. Upon examination of the remainder of the comparative plots, the behavior appeared to be consistent throughout as there seemed to be almost regular trends of polarity reversals in each of the ten sets of charts. As in the skim 0 comparison, each other skim seemed to correlate most strongly with skim 9 and 10, the ones farthest away. Skim 5, however, did not seem to strongly correlate with any of the other skims as each plot exhibited a random display of points. Examination of the raw skim 5 data revealed uncharacteristic signal behavior that was likely not the result of geophysical or geological variations. With respect to all of the fifty-five comparisons from the bottom sensor data, an average R^2 of .282 resulted. This means that for each calculated trend, only about 28% of the data points were in agreement.

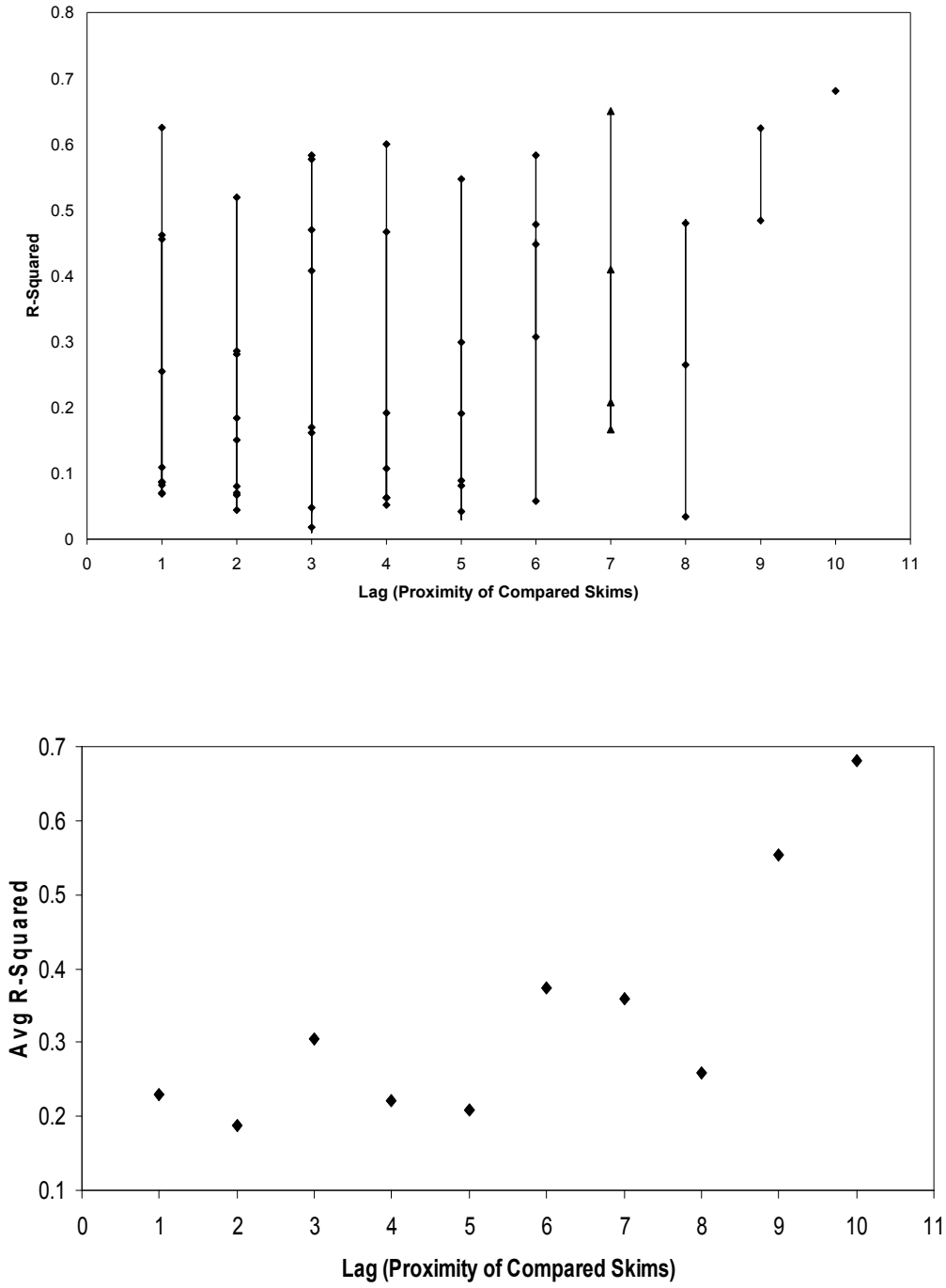

Figure 14. Bottom sensor r-squared values for each of the magnetics amplitude analysis plots with respect to the lag of the compared skims. Average r-squared values for each lag were calculated from the first chart and plotted on the lower chart.

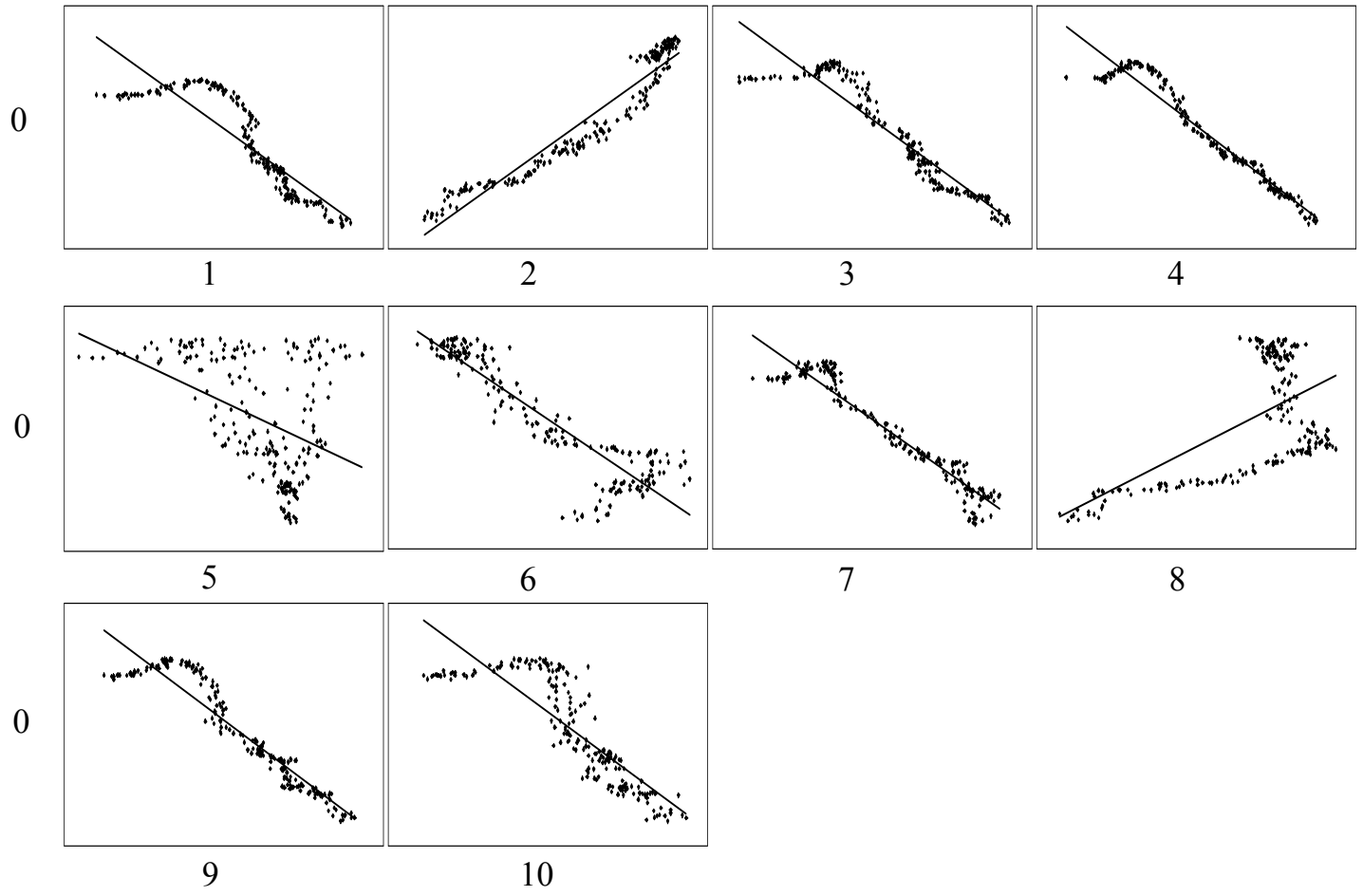

Figure 15. Example of top sensor amplitude analysis results as skim 0 magnetics data are plotted against the equivalent data from skims 1 through 10.

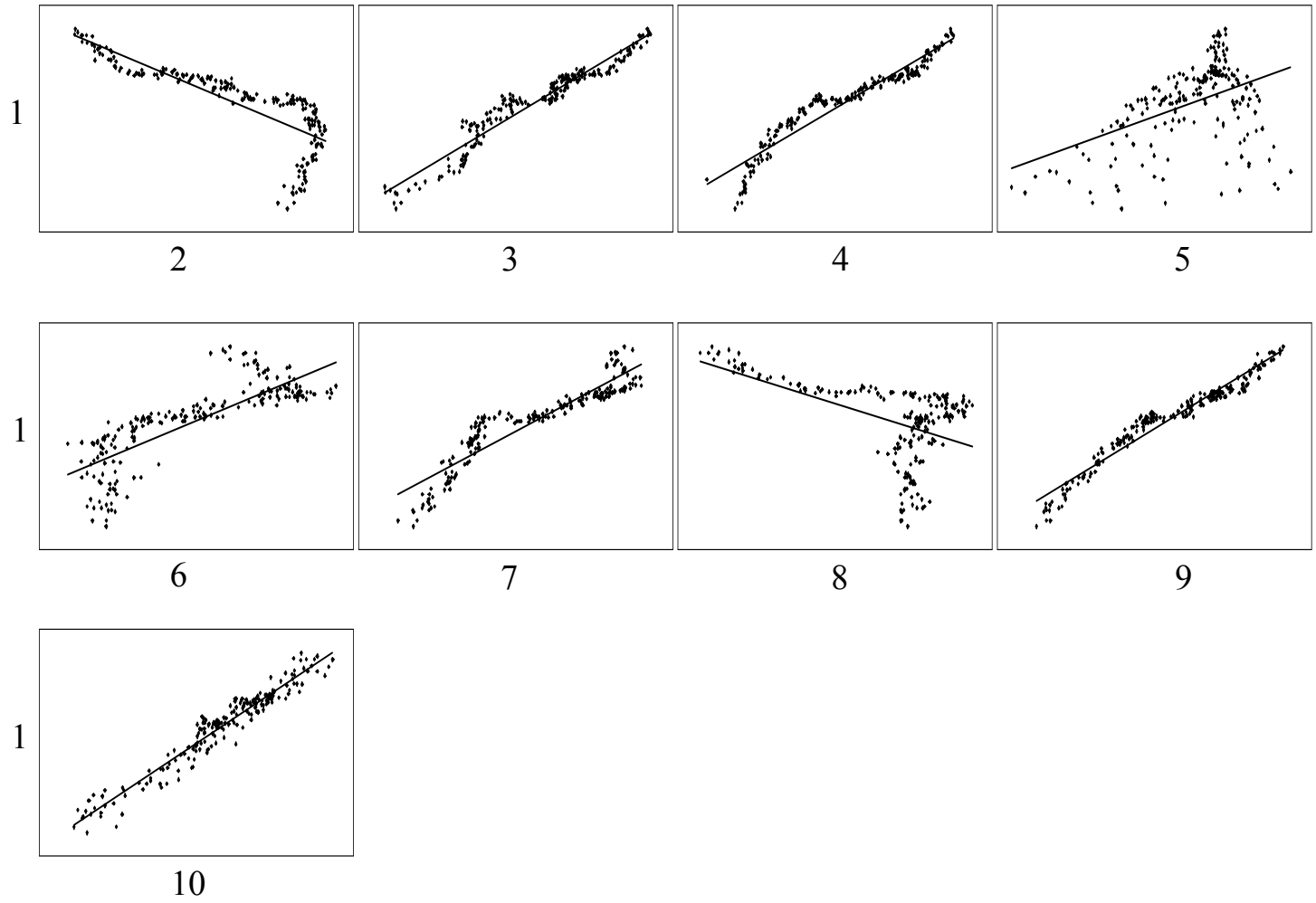

Figure 16. Example of bottom sensor amplitude analysis results for skim 1 magnetics data are plotted against the equivalent data from each subsequent skim.

Amplitude Analysis: Top Sensor

To gain a better understanding of the magnetics data, the same analysis was performed with the values from the top sensor to ensure that there were no procedural errors in the previous operation that resulted in the unexpected findings (Figures 15 and 16). It was expected that the top sensor data would mimic that of the bottom sensor as they were essentially recording the same magnetic variations. The difference, however, is that the top sensor is influenced primarily by heterogeneities deeper in the subsurface while the bottom sensor, being closer to the earths surface, was more susceptible to very small scale perturbations at shallower depths. Because of this, the top sensor data was hypothesized to possess greater correlative values as the deeper heterogeneities influencing the top sensor are not disturbed by the skimming process.

Amplitude Analysis: Top Sensor Results

As predicted, the top sensor showed more consistency between skims. While the bottom sensor averaged a 28% trend agreement, the top sensor plots resulted in an average R^2 of .613, or 61% agreement (Figure 17). Despite the large increase in the strength of the correlations, the nature of the trends remained enigmatic in that the polarity variations were seen in these data exactly as they were seen in the bottom sensor data but with greater clarity and definition.

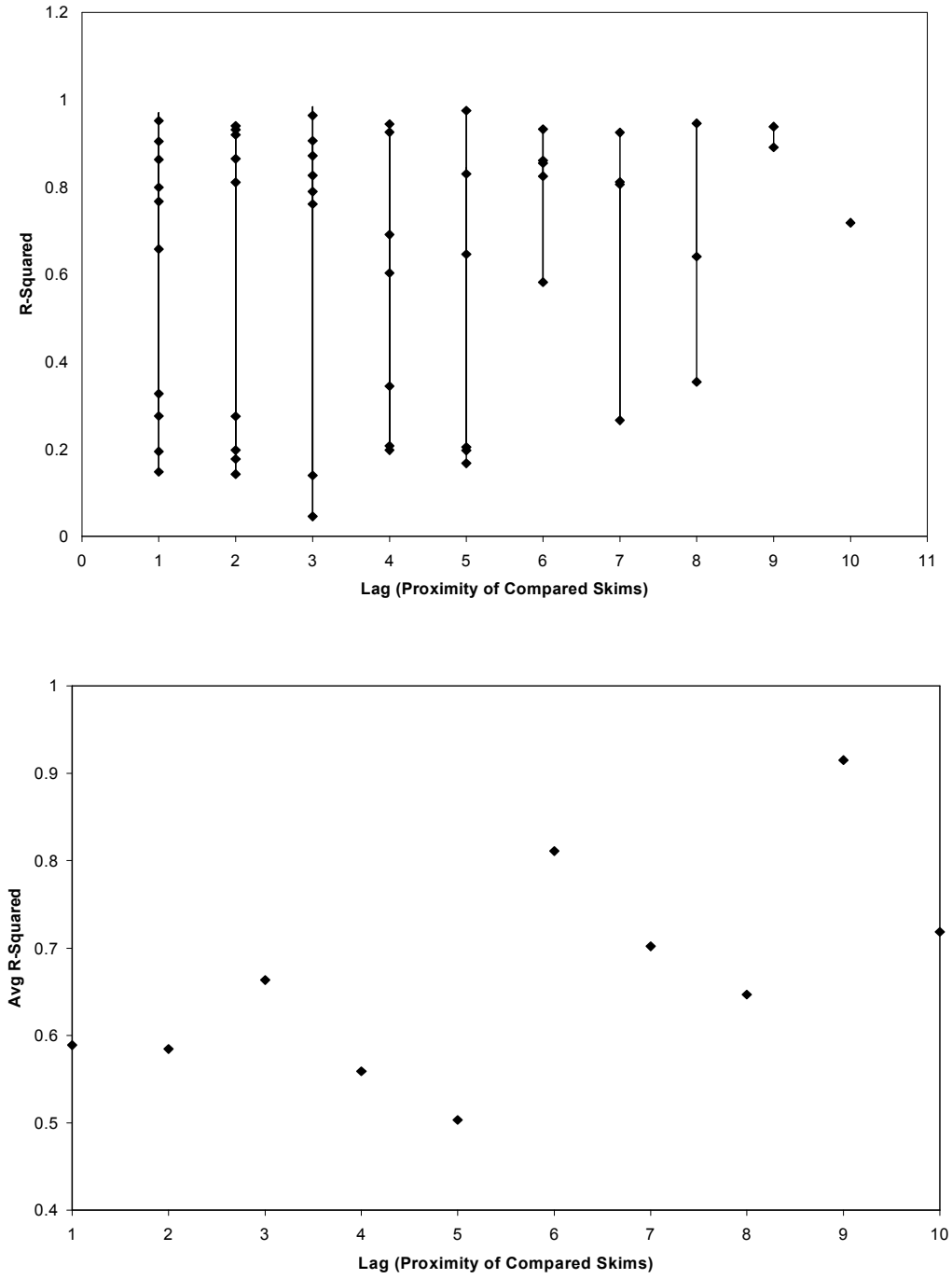

Figure 17. Bottom sensor r-squared values for each of the magnetics amplitude analysis plots with respect to the lag of the compared skims. Average r-squared values for each lag were calculated from the first chart and plotted on the lower chart.

GROUND PENETRATING RADAR

Introduction

The GPR component of the experiment was designed with the intention of acquiring a background dataset along the survey line prior to the removal of any material. However, as a result of unexpected technical difficulties and time constraints the initial GPR data collection did not take place. When the GPR was assembled at the experiment site, it was discovered that, while the transmitter antenna appeared to be responding, the computer was not registering a signal from the receiver antenna. The batteries were checked to ensure they were sufficiently charged and each connection from the computer to the console and the console to the antennae was examined. Further troubleshooting revealed that the instrument console, which had occasionally been problematic for users in the past, was not functioning properly. As time was an issue, from equipment rental and personnel perspectives, it was decided that the experiment would continue and that the GPR would be incorporated as soon as it was in working order. Fortunately, another Pulse_EKKO 100 instrument was available from the geology department, and the console from that instrument was substituted into the initial system and ultimately proved to be the solution to the problem. By this time, the initial skim had taken place, not allowing background GPR data to be collected. A profile was run, however, after the first skim along the 50 m survey line with a station interval of .5 m. Upon examination of the collected data, it was decided that in order to achieve the

desired level of data resolution for this experiment, the spacing between measurements should be decreased from .5 m to .25 m. The .25 m station interval was used for skims 2 through 10, which was the final survey of the experiment. As a result of the changes brought about by technical issues and design reevaluation, the GPR data analysis involved skims 2 through 10 only as they contain an equal number of traces and measurements that were taken at the same locations along the survey line.

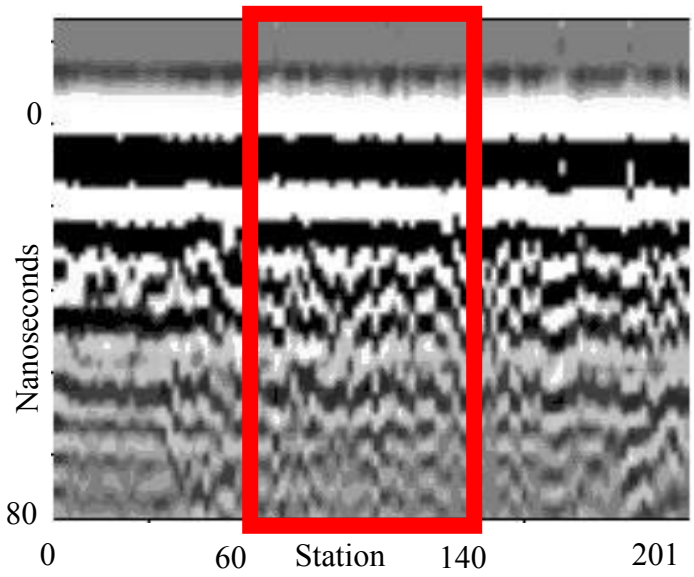

Figure 18. Example of a GPR data section with the data used in the analyses encompassed in the box.

Because the intent of this experiment is to examine data collected as the near-surface material is removed, it was not necessary to analyze each of the 201 traces along

the 50 m survey line. Instead, only the data collected between the 15 m and 45 m marks, or GPR traces 60 to 140, were used as highlighted in Figure 18. This range was selected because it includes a sufficient quantity of data to support the presence or lack of trends produced by the analyses and the 15 m and 45 m location are believed to be far enough away for the trench ramps not to have a significant influence on the data.

Preliminary Data Processing

Before the GPR data could be analyzed and processed, several tasks had to be performed. The first task was to convert the raw data .dat files into .xls files that could be viewed in spreadsheet form in Microsoft Excel. Each of the nine raw text files was converted and then compiled into one master spreadsheet composed of nine columns to make easier the future analysis and comparison operations. To further improve ease of data manipulation, all extraneous information was removed, including the 161 traces outside of the interior 20 m of the trench. The spreadsheet then contained only the traces of interest from each skim, and served as the initial file for all subsequent operations performed on the GPR data. Before the data could be analyzed, however, random traces from each skim were plotted to check that the time-zero, or first amplitude break, occurred at the same time. The evaluation showed that the traces comprising the skim ten dataset exhibited a first-break roughly thirteen sample points earlier than those of the previous eight skims. This means that the instrument began recording each trace at a later time on skim ten, which resulted in thirteen fewer sample points before the first

signal arrived at the receiver antenna. To correct this problem, the initial thirteen sample points were removed from each of the traces on the previous skims, effectively shifting each feature in each trace up thirteen samples in the section. A result of the shift, each dataset other than skim ten then had thirteen fewer sample points at the end of the section. To achieve uniformity, the last thirteen sample points on the remaining eight skim traces were cut from the sections, creating a time-zero corrected section composed of 87 samples instead of the original 100 (Figure 19)

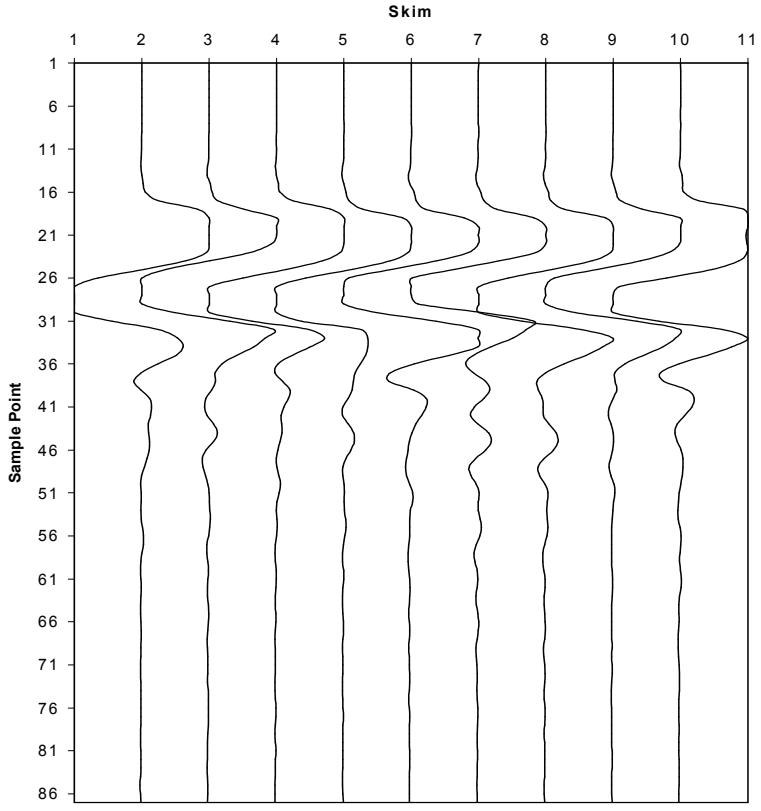

Figure 19. GPR trace from station 60 from each skim after time-zero correction.

This was an important measure in that it adjusted each skim to a common datum, which allowed for accurate comparisons to be made between data from different skims. Upon completion of the above tasks, the data were then in a format that could easily be used for manipulation and plotting.

Average Amplitude Analysis

The first operation used to analyze the GPR data was based on amplitude variations in individual traces. This was done to reveal any obvious trends or correlations in the data. The first step of this process was to identify a manner in which data from one skim could be accurately compared to the equivalent data, from both a spatial and temporal perspective, a different skim. The spatial aspect of this problem was easily solved in that each survey following a skim used the same station interval, which means that the station numbers for each skims correspond to same locations along the survey line (e.g. trace 60 in the second skim was made at the same location as trace 60 in the following eight skims, with the elevation being the only variable). Secondly, because the strong amplitudes produced by near-surface effects in the trace needed to be excluded, a *window* was defined for each trace, denoting the portion of the trace to be included in the analysis. The borders of the window were defined by sample numbers chosen a sufficient time from the near-surface effects, such that they had no influence on the data. The window for the first analysis included sample points 60 to 80, near the end

of the trace (Figure 20). This includes roughly 25% of the information contained in each trace, and served as an adequate starting point for the data comparison.

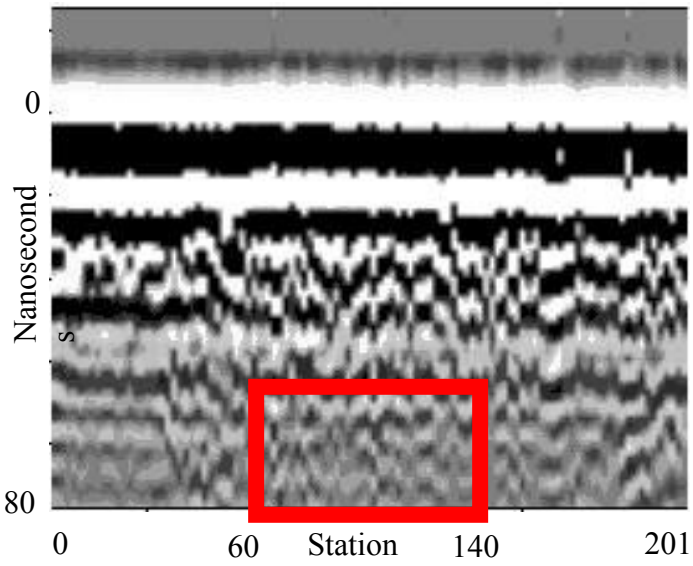

Figure 20. GPR section with the 60-80 ns analysis window highlighted.

A new spreadsheet was created specifically for this operation. The first manipulation involved removing the initial 59 and final 7 sample points on each trace, leaving only the selected 60 to 80 point window. Secondly, because this analysis dealt only with amplitude variations and not exact, recorded values, the remaining data were then normalized to sample 60 in each trace. This was done by simply subtracting the measured value at sample 60 from each of the twenty-one samples in that trace. The result was a value of zero at the first sample of each trace followed by small values at the

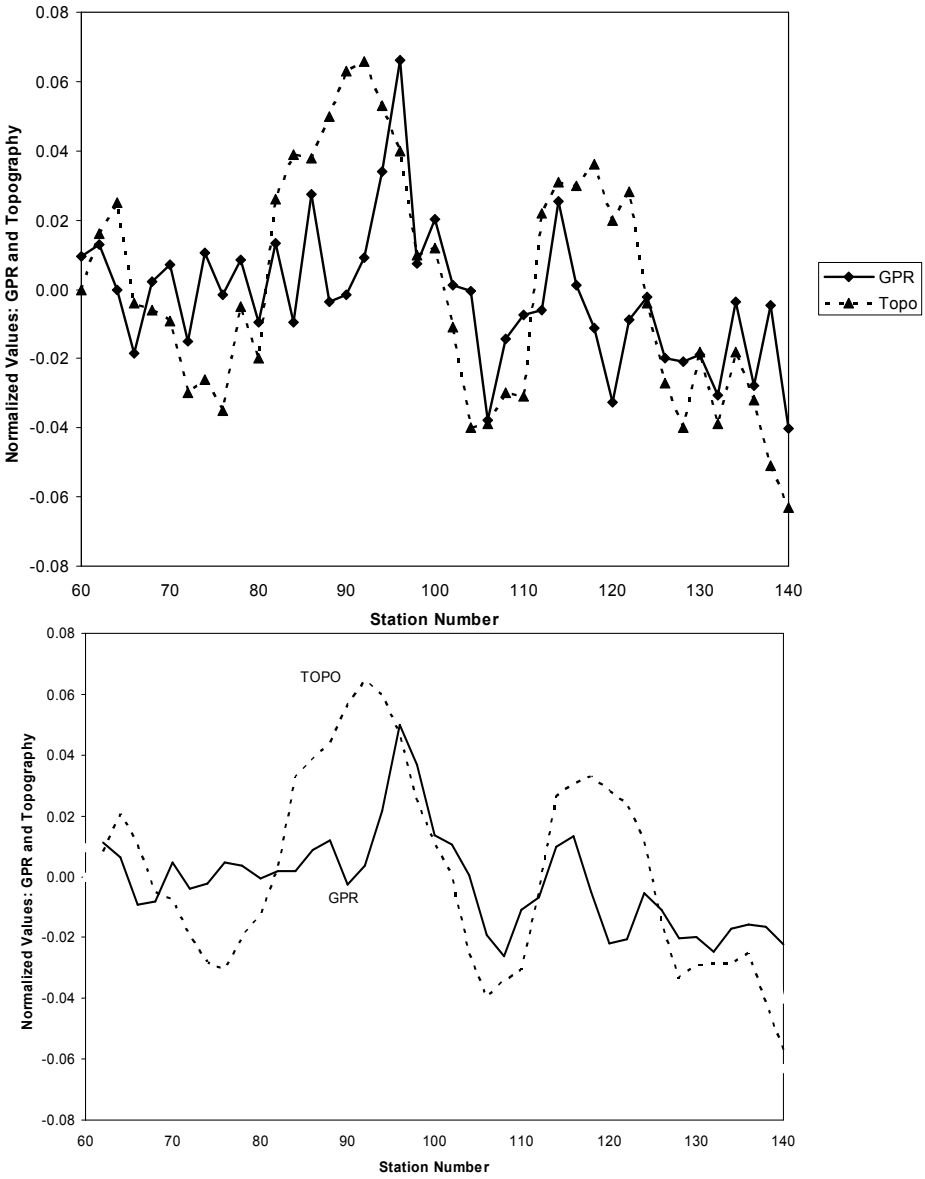

Figure 21. The top chart shows skim 3 data changes in topography and average GPR amplitude over the analysis region while the lower chart plots a running average.

subsequent points representing the numerical difference from sample 60. Then, having only the normalized values for the predetermined window, the average of the twenty-one values for each trace was calculated. This operation was performed on traces 60 to 140, which covers portion of the trench to be analyzed, for each of the eight skims yielding 81 average amplitude values for each skim.

First, the average amplitude data were used to identify any possible relationships between GPR response and variations in micro-topography. This was done by creating a plot for each skim with both GPR and topography data represented. Because the .25 m station interval for the GPR survey differed from the .5 m interval of the topography survey, only the values that corresponded directly with the topography values were used. This effectively eliminated the GPR data collected at all .25 and .75 m locations. Thus, the remaining 40 GPR values were plotted against the 40 topography values for each of the eight skims in both line and scatter chart formats. The line chart plotted two series, one representing the GPR average amplitude and the other the topography data (Figure 21). This format provided a visual comparison of the variances of each data type. The scatter plot displayed the average amplitude values as the y-axis values and the collected topography data for the x-values. This was done to graphically identify any trends or relationships between the two datasets.

Secondly, a series of scatter plots was created to directly compare the average amplitudes from each skim to one another. Using all of the GPR traces, the 81 average amplitude values from skim 2 were plotted as the y-axis values for ten individual graphs. The x-axes on these ten scatter plots were composed of the calculated values from skims

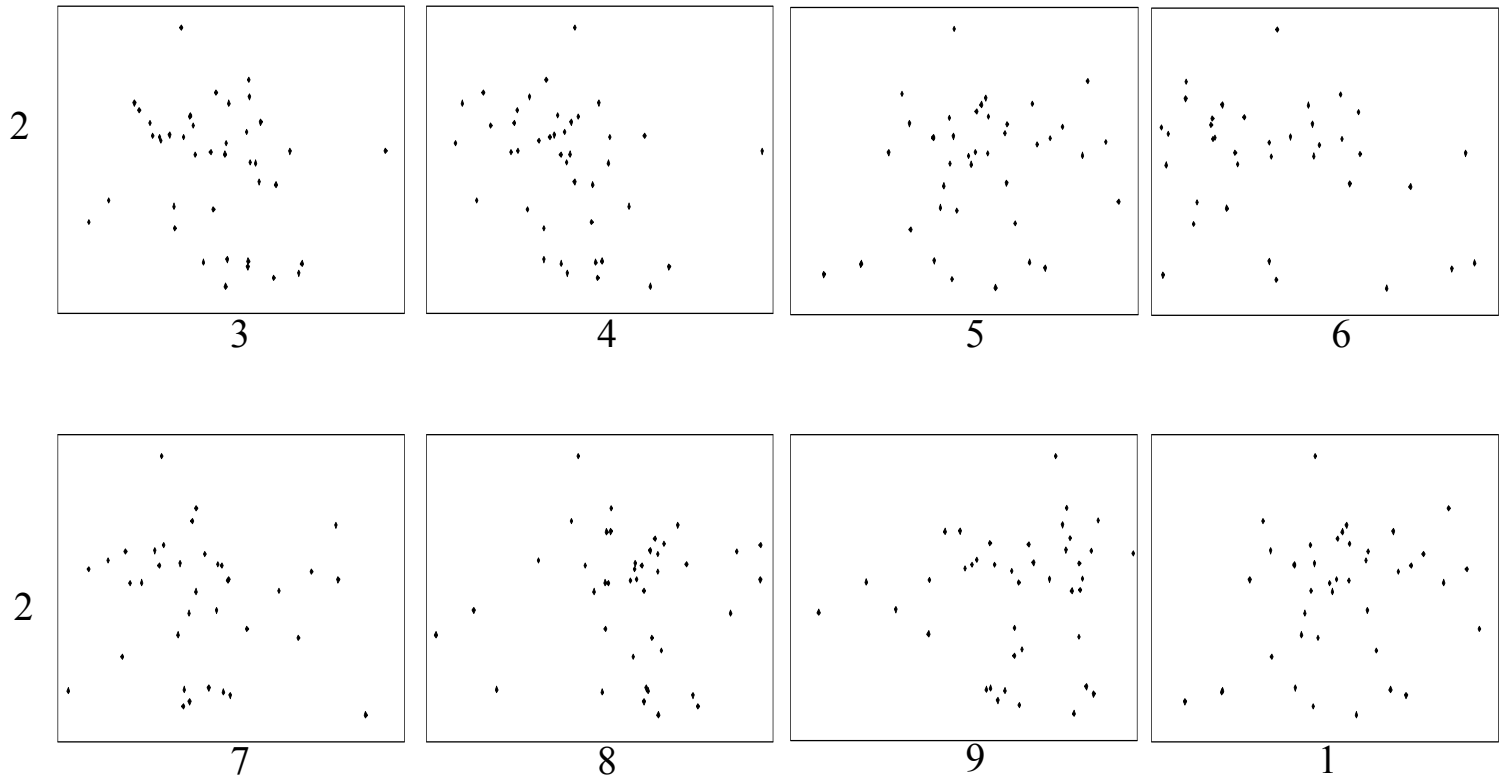

Figure 22. Example of GPR average amplitude analysis results for skim 2 data plotted against the equivalent data from each subsequent skim.

3 through 10, respectively, with the skim 2 results being shown in Figure 22.. This was repeated for y-axis values of skims 3 through 9, for a total of 36 plots. The process was conducted in this manner so that each skim would be compared not only to adjacent skims, but to every other skim in the experiment. Again, this type of display was used to show any trends that may have been present in the data as a function of skim lag.

Average Amplitude Analysis Results

Upon examination of the numerous plots created with respect to amplitude and topography, some preliminary interpretations were made. First, the line-graphs were considered in order to visually identify any trends that may be present. The initial observations were made to determine if there was an apparent direct or inverse relationship between the two datasets. A direct relationship would have resulted in corresponding peaks and troughs in the two series while an inverse trend would cause peaks in one series associated with a trough in the other and vice versa. Looking at the graphs, a minor direct relationship was seen in the areas of the chart where the deviations were greatest while there appeared to be little or no coherence in the subtle variations.

This suggests a weak direct relationship between the two series occurring only when large variations in topography are present. To further substantiate these findings, a running average with a period of 2 sample points was applied to each dataset in hopes that resultant curves would be similar in nature (Figure 21). A deliberately small period was chosen to preserve the greatest amount of character of the initial data. A visual assessment of the running average curves again noted a weak direct relationship between the average amplitude values and the topography data. To add statistical insight to this interpretation, the scatter plot was used. With the GPR data plotted against the topography data, a direct relationship would be evidenced by a consistent upward sloping trend of data points. Initial review of the data, however, only showed a viable relationship on two of the eight plots. A linear regression was done for each skim and the R^2 values for each trend line were calculated. Each regression produced a trend line with a positive slope, while the R^2, or the suitability of the line to the data, ranged from .0008 to .3014. Skim 4 and skim 8 showed a significant correlation with topography with R^2 values of .3014 and .2656 respectively, which effectively means that 30% and 26% of the data points were in agreement with the trend line.

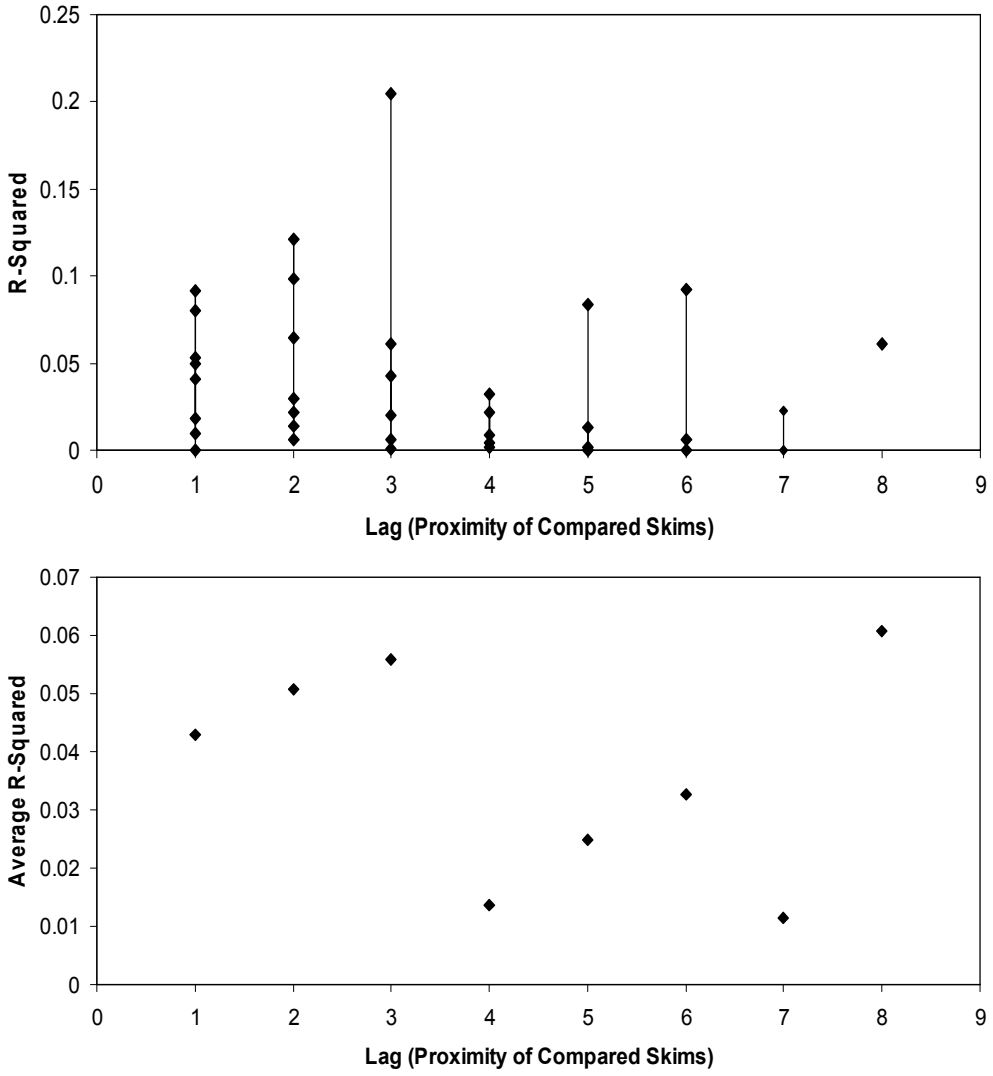

Figure 23. R-squared results from the average amplitude analysis in the 60 to 80 ns window.

The second series of graphs that plotted the average amplitudes of each skim against one another as a series of points yielded very similar results. It was thought that the skims that were compared to nearby skims (low skim lag) would possess some kind or relationship and that the relationship would dissipate with the comparison of skims further apart from one another (large lag). The data, however, did not support this idea. Each plot, regardless of the proximity of the two skims being compared, seemed to display a random pattern with no features that accurately correlated (Figure 23). It was thought that perhaps the analysis window from sample points 60 to 80 was too deep in the trace to effectively measure signal amplitudes and may have, in fact, been dominated by noise. To test this hypothesis, the analysis window was moved up to include sample points 40 to 60 which begins at the terminus of the near-surface effects (Figure 24). These plots, however, also exhibited a random data display, similar to the type seen in the previous analysis window (Figure 25).

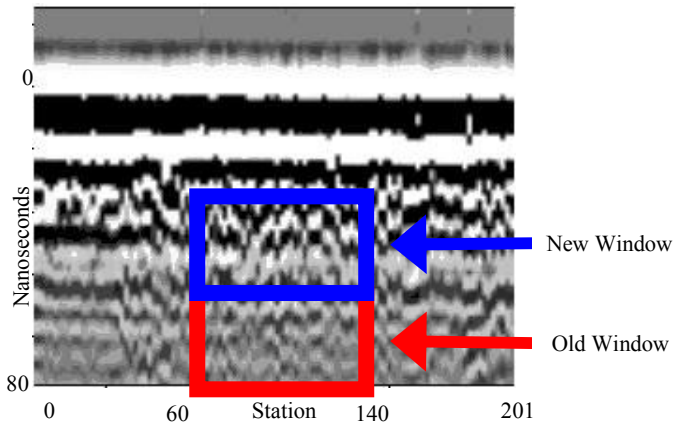

Figure 24. The second average amplitude analysis was performed using data from an earlier time window, 40 to 60 ns.

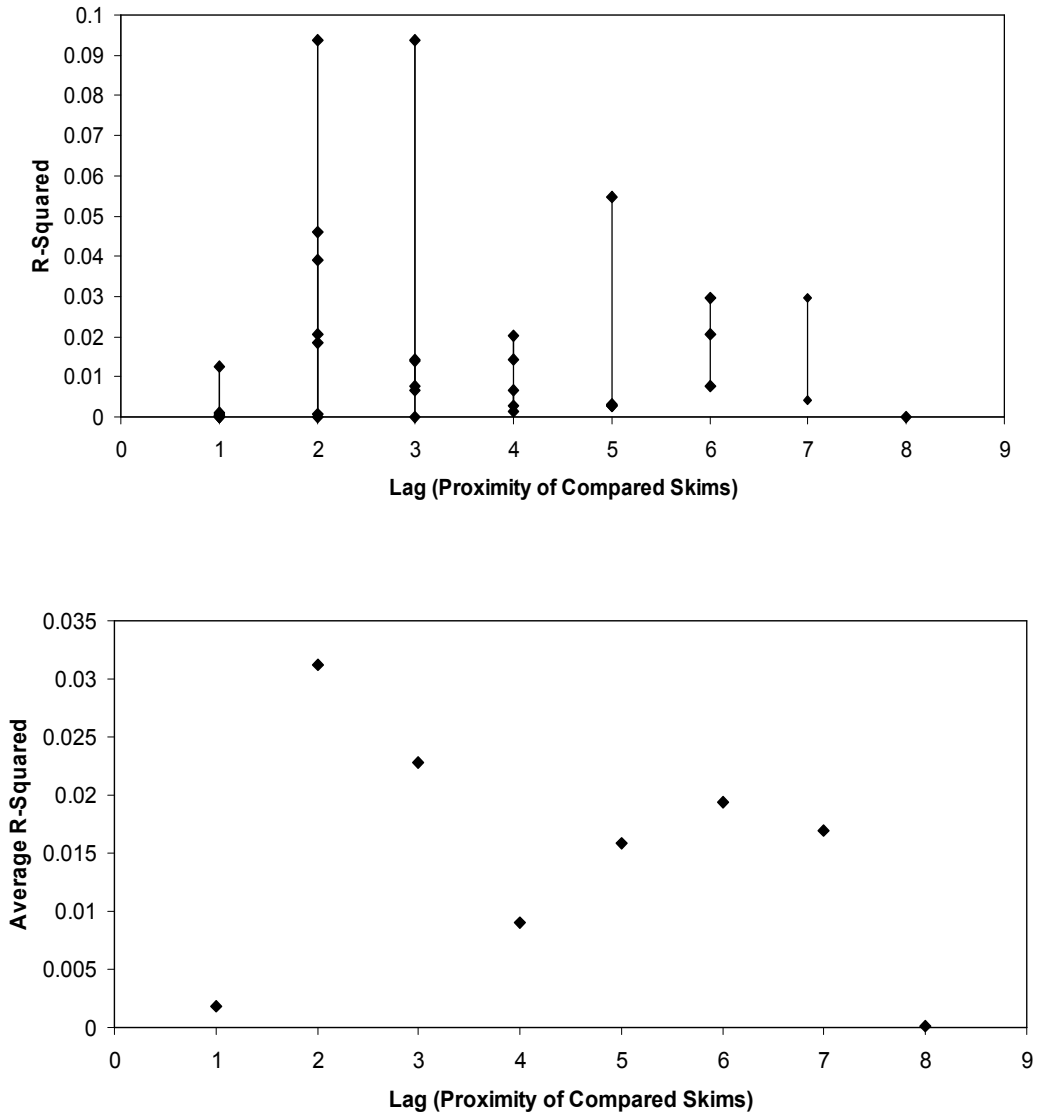

Figure 25. R-squared results from the average amplitude analysis in the 40 to 60 ns window.

Graphical Amplitude Correlation

Since no definitive relationships were found in the previous two analyses, a different approach was taken for the final operation. Here, a single trace was taken and directly compared to the traces from the same station number of the remaining eight skims (Figure 26). The intent was to determine if particular amplitudes could be tracked up in section as the near-surface material was progressively removed, thus giving evidence of how the signal changes as a result. The method is somewhat analogous to well-log correlation in petroleum geology and geophysics where signals produced by subsurface lithologies are tracked between logs from differing locations. Initially, trace 60 from each skim was plotted to the same scale and positioned next to one another a uniform distance apart. Immediately, it was observed that the near-surface effects saturated the plots as the amplitude variations below were not readily visible. To correct for this, the traces were cropped to display sample points 50 to 87, from just below the large near-surface amplitudes to the end of the trace. The traces could then be normalized to sample point 50 and plotted on an adjusted scale to enhance the amplitude variations of interest. The same procedure was carried out for traces 70, 80 and 90 and each were printed on a 20 x 12 in plot so that even the most subtle variations could be observed. Each set of traces was examined and lines were drawn between traces to connect amplitudes interpreted to be the same. For this operation the topography data were important as the quantity of material removed at each station after each skim

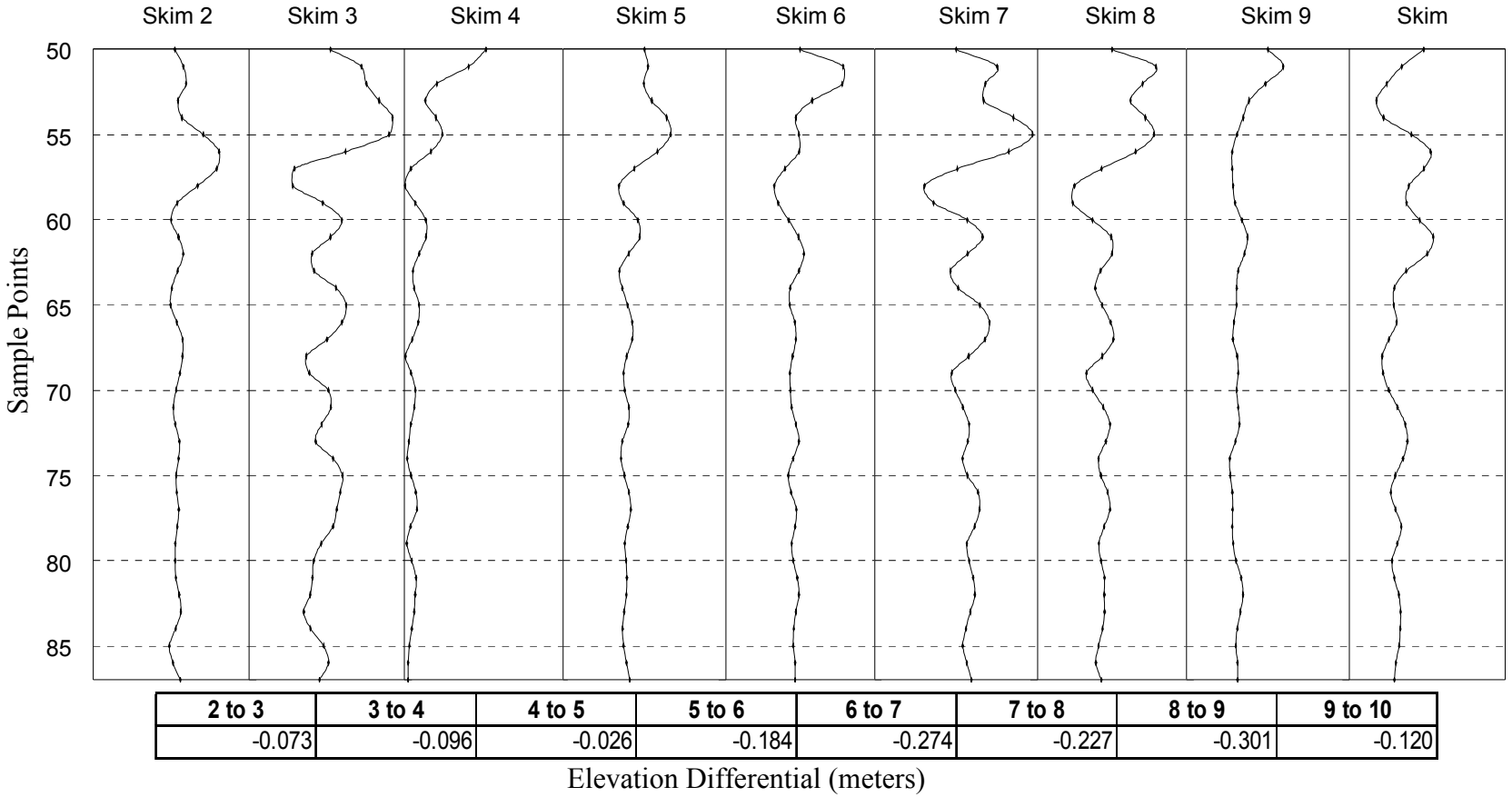

2 to 3	3 to 4	4 to 5	5 to 6	6 to 7	7 to 8	8 to 9	9 to 10
-0.073	-0.096	-0.026	-0.184	-0.274	-0.227	-0.301	-0.120

Elevation Differential (meters)

Figure 26. GPR trace 60 shown for each skim with the elevation change from one skim to the next at that station.

theoretically governed the degree to which a particular amplitude would be shifted in time. As a rough guide for this correlation, the amount of shift expected to occur after a skim was calculated. This was done using the equation

$$t = \frac{2d}{v}$$

where v represents the velocity of the GPR wave through the medium and d and t represent the distance traveled by the wave and the two-way travel time respectively. The distance was simply the change in elevation between the two skims being compared at the station of interest and was found from the topographic data. Multiplying the elevation difference by 2 was necessary because the recorded wave had traveled down to the reflector and back up to the receiver. The velocity used was 10^8 m/s or $c/3$ where c represents the speed of light. This value is accepted as the standard velocity for EM wave propagation through general earth materials with RDP~9. The resultant values of time from this equation are in s. The traces were plotted with respect to sample number instead of time or depth, so a conversion needed to be made. The GPR specifications indicated that sample points are recorded every .8 ns, or 8×10^{-10} seconds. Knowing this allowed the time given from the equation to easily be expressed in terms of sample numbers, which allowed for a rough approximation of how many sample points any given trace feature should be shifted from one skim to the next.

Graphical Amplitude Correlation Results

The beginning of the correlation process on trace 60 went very smoothly in that the measured shift appeared to be the same as the calculated shift and the features in each of the traces could be associated to one another with a high degree of confidence (Figure 27). There was .073 m of material removed from station 60 from skim 2 to skim 3. Using the above formula, it was calculated that trace 60 of skim 3 should be translated up 1.4 ns, or 1.8 sample points, with respect that the same trace from skim 2. As expected, each feature correlated from skim 2 was shifted up two samples points in skim 3. By the same process, the change from skim 3 to skim 4 was predicted to be on the order of three sample points. From the chart, however, a shift of five points was observed consistently throughout the traces, which would suggest a velocity closer to $c/6$. Giving the same attention to each skim for traces 70, 80 and 90 resulted in similar findings. While in some instances amplitudes correlated very well with one another and exhibited a shift close to what was expected, other traces seemed to display a character completely different from those of other skims (Figure 27). The comparisons were even more ambiguous when analyzing the later skims due to the fact that substantially more material was removed during skims 7 through 9 than during the earlier skims. It is believed that the inconsistent and dramatic variations in trace character from one skim to the next are primarily resultant of survey design flaws. GPR data are very sensitive to the conditions in which they are collected, including how well the antennae are coupled

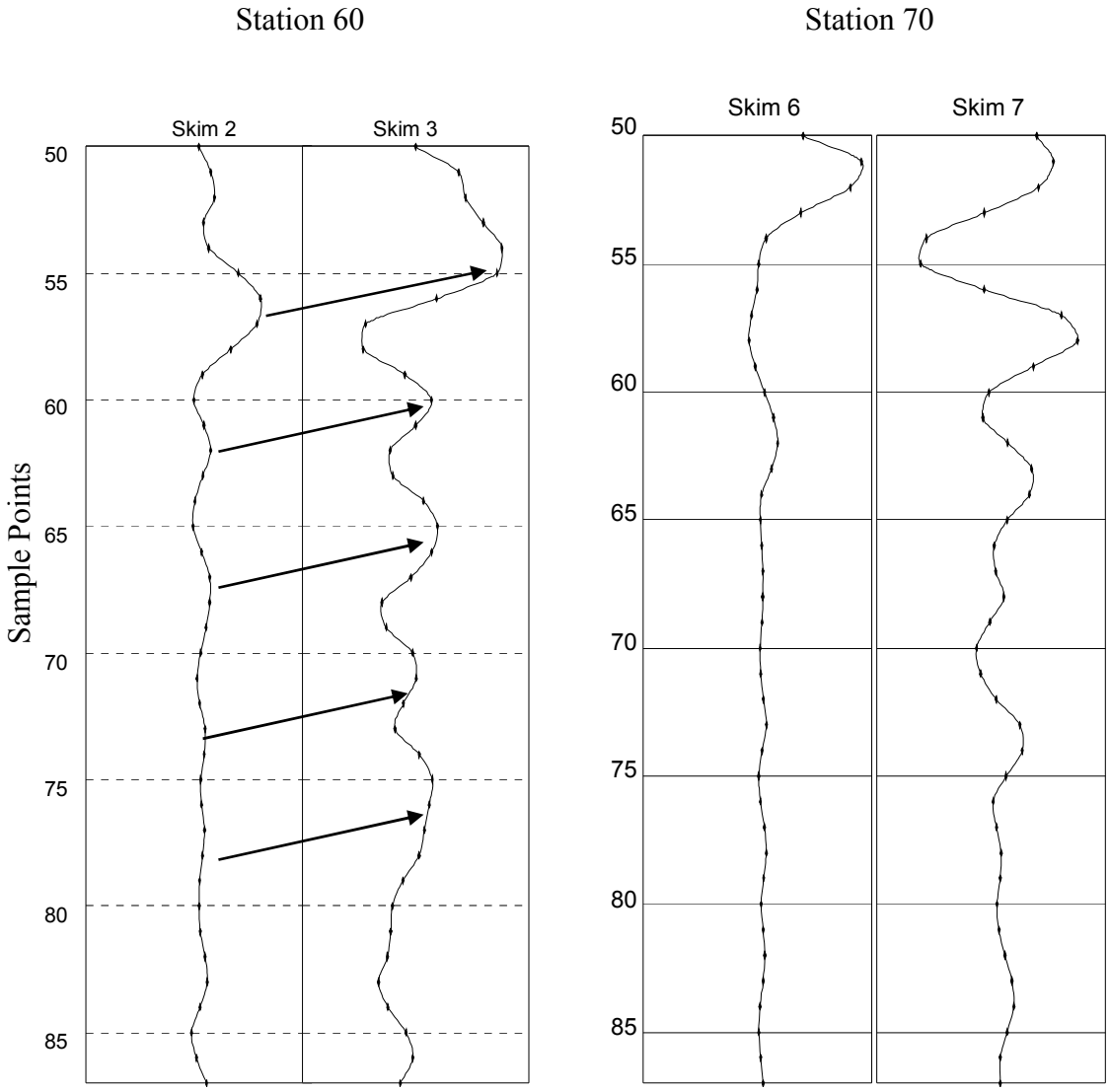

Figure 27. GPR trace from station 60 from skim 2 to 3 with corresponding anomalies noted and the trace from station 70 from skim 6 to 7 showing very little similarities.

to the ground as well as the attitude or orientation of the antennae with respect to one another. As more material was removed with each skim, the trench area became progressively more uneven and rugged with the presence of clumps of dirt that, at times, obstructed antenna contact with the ground. These conditions caused slight changes in the position of the instrument when measurements were being taken and ultimately resulted in inconsistent data quality.

ELECTROMAGNETIC INDUCTION

Introduction

For ease of operation during data acquisition, some modifications were made to the EM-63 as it was not used in the cart-mounted configuration for which it was designed was not well suited to the trench acquisition. The receiver coil was placed inside of the transmitter loop at ground level. In order to couple the two components of the instrument and for ease of movement along the survey line, the EM-63 and battery pack were secured to two 2x4 in wooden boards to create a sled-type configuration. The instrument could then be easily operated by two individuals with one pulling the sled from one station to the next and the other following shortly behind holding the console and recording the measurements.

The first EM data were collected prior to removal of any material to acquire a background dataset, as was done with the other instruments. Beginning at the 0 m point of the survey line, data points were collected every .5 m for a total of 101 measurements per skim. This process was repeated after skims 1 and 2. For the remaining skims, however, the station interval was decreased from .5 m to .25 m, doubling the amount of readings taken for each skim to 201. This decision was made because the data collection was going more rapidly than expected and increased resolution of the EM response inside the trench was desired. The collection of EM data throughout the entire experiment was free of any problems or complications and full datasets were gathered

for each of the ten skims and the background. The survey did become slightly more difficult and time-consuming, however, as the trench became deeper and the topography more irregular making the repositioning of the sled more laborious.

Preliminary Data Corrections

Prior to any analysis, the data were organized and slight modifications were made where necessary. The dataset from each skim was imported into a spreadsheet and plots were made to graphically represent the signal. An initial overview of the data revealed the presence of a recurrent, anomalous spike (Figure 28). The fact that the feature was uncharacteristic of the remaining data and that it vanished after the fourth skim, suggested that it was non-natural in origin. It was likely due to a metallic object that was indeed ultimately removed from the survey line with the material excavated during skim 5. It was important that the artifact did not influence the data, so it's effect was removed from each dataset using the information on either side of the spike. A similar peak was noticed in skims 8 and 9 and was removed in the same fashion.

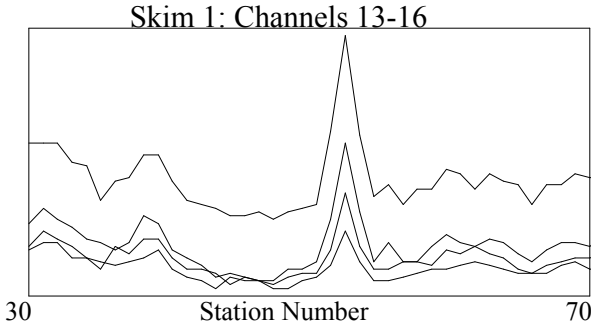

Figure 28. EM data from skim 1 showing the anomalous spike believed to be the result of a foreign metal object in the survey area.

The data were then sorted such that only the measurements from stations within the interior 20 m of the trench remained. For the first three datasets, skims 0 through 2, stations 30 to 70 were of interest as the station interval was .5 m. Stations 60 to 140 were retained for the remainder of the skims where the spacing between measurements was decreased to .25 m. A copy spreadsheet of each of the skims with .25 m spacing was made and every other station (those not located at meter or half-meter marks) was removed so that a direct comparison could be made with data from the first three skims.

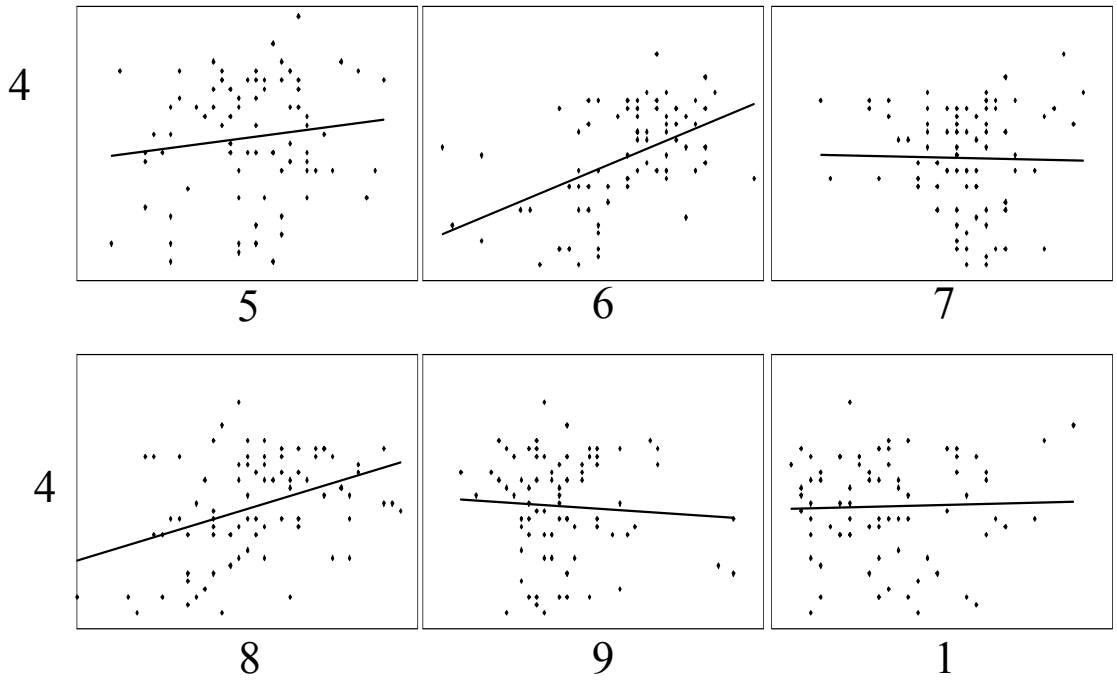

Figure 29. Example of EM amplitude analysis results for skim 4 channel 1 data plotted against the equivalent data from each subsequent skim.

Amplitude Analysis

As with the magnetics and GPR data, an analysis was performed to examine how amplitude changes in the data related to changes in each of the other skims (Figure 29). Unlike the other datasets, however, each EM set was composed of 26 values per station as data were collected at 26 logarithmically spaced time intervals. As a result, analyses had to be done with respect to a particular time channel. Trial analyses found that there was too little variation in the very early and very late time data to produce useful results. Data from channels 1, 6, 12 and 16 were used for the comparisons. An analysis was performed for each of the three channels in order to ensure that the results were consistent throughout the data and did not vary significantly from one channel to the next. In each analysis, all data compared with skims 0 through 2 employed values from the 41 stations collected at .5 m intervals which the later skims used all 60 values

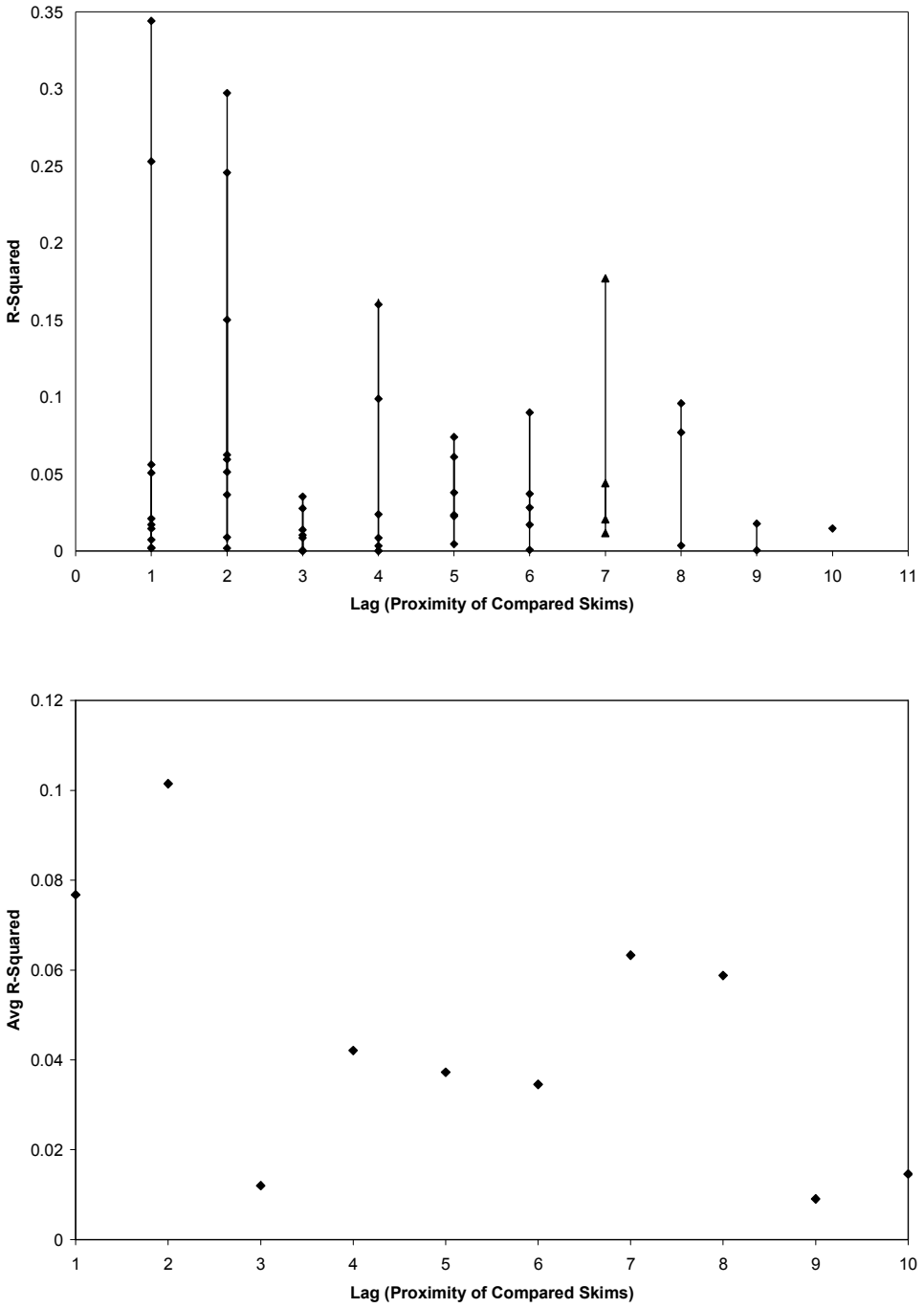

Figure 30. R-squared results for channel 1 EM amplitude analysis.

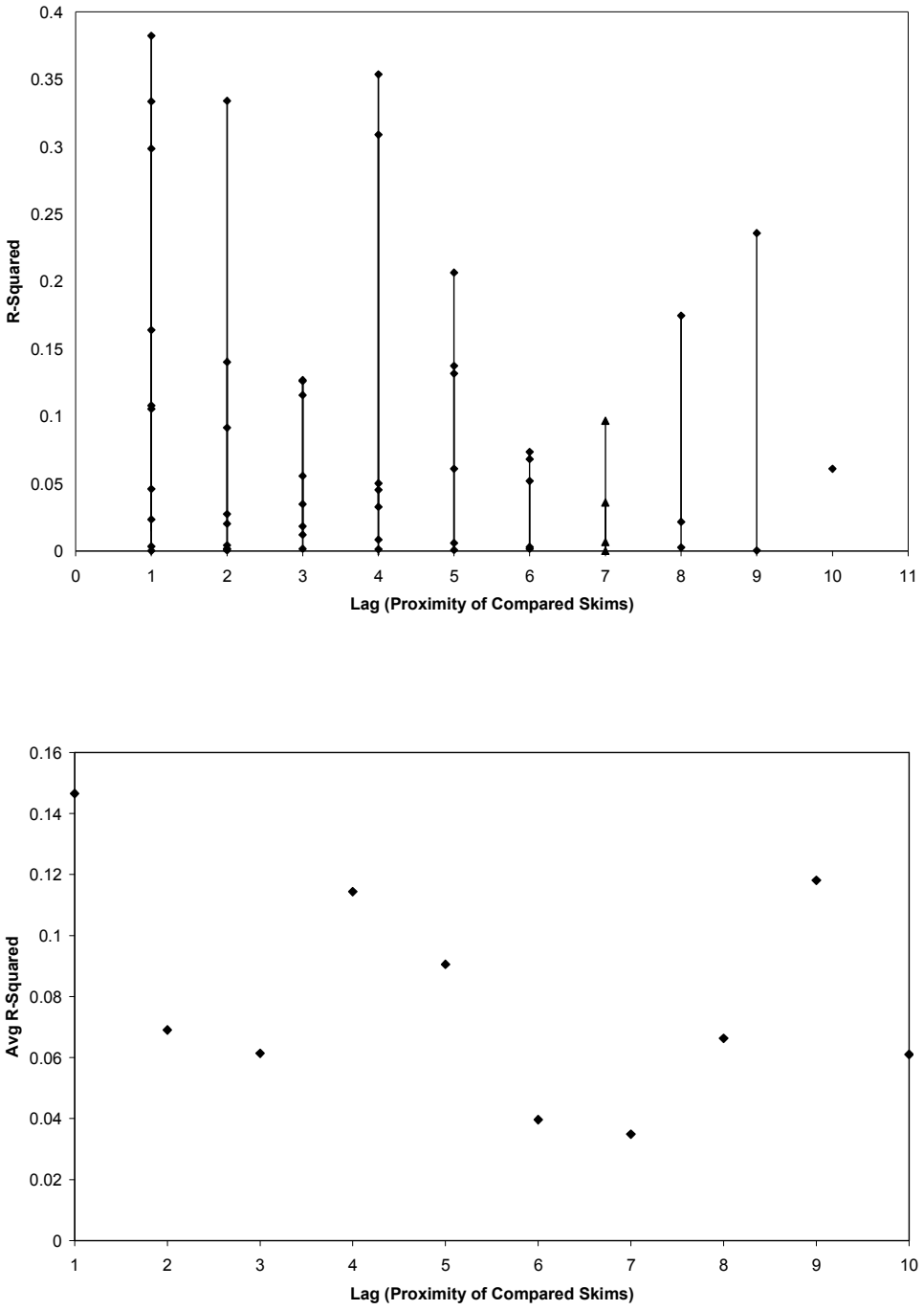

Figure 31. R-squared results for channel 6 EM amplitude analysis.

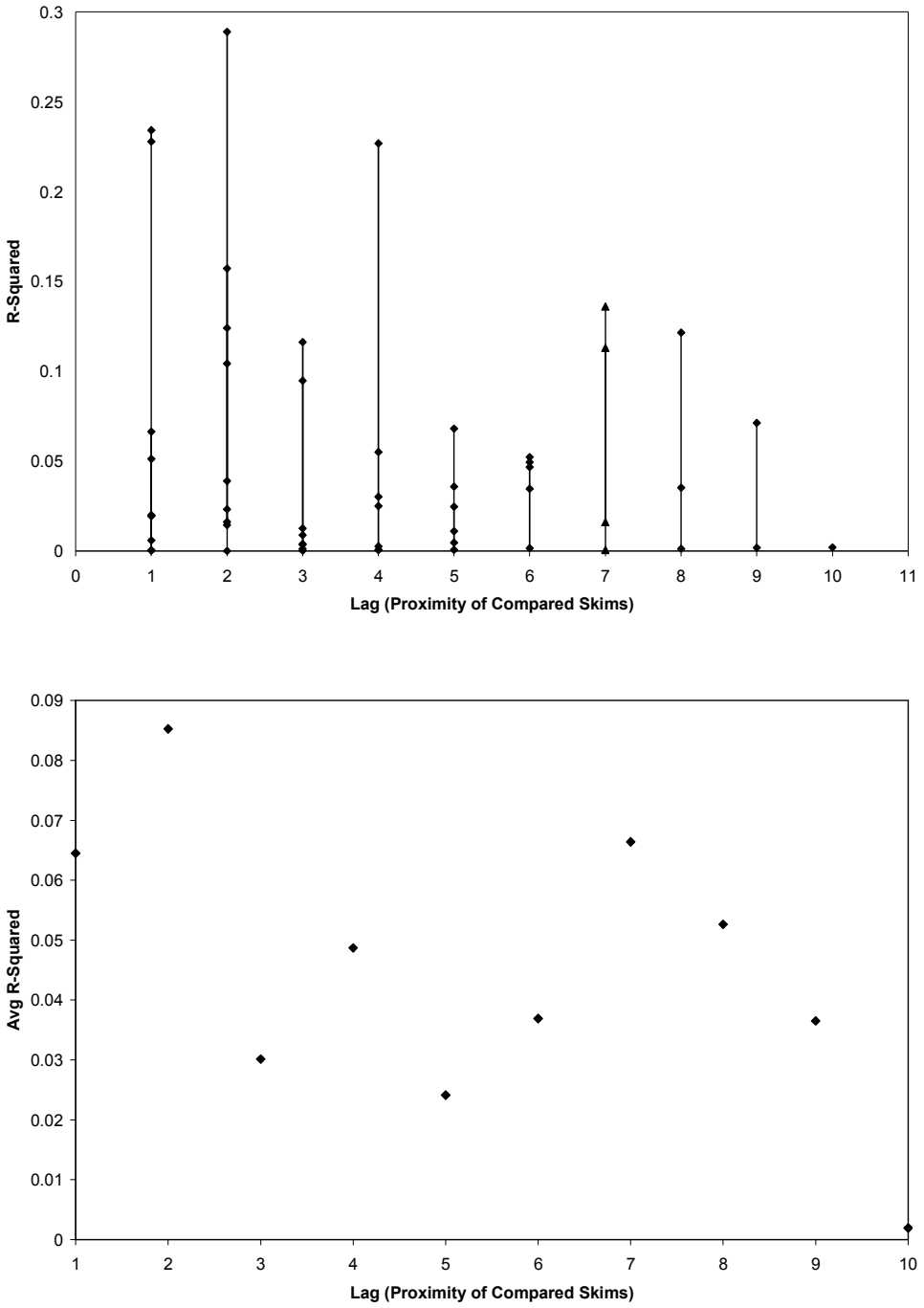

Figure 32. R-squared results for channel 12 EM amplitude analysis.

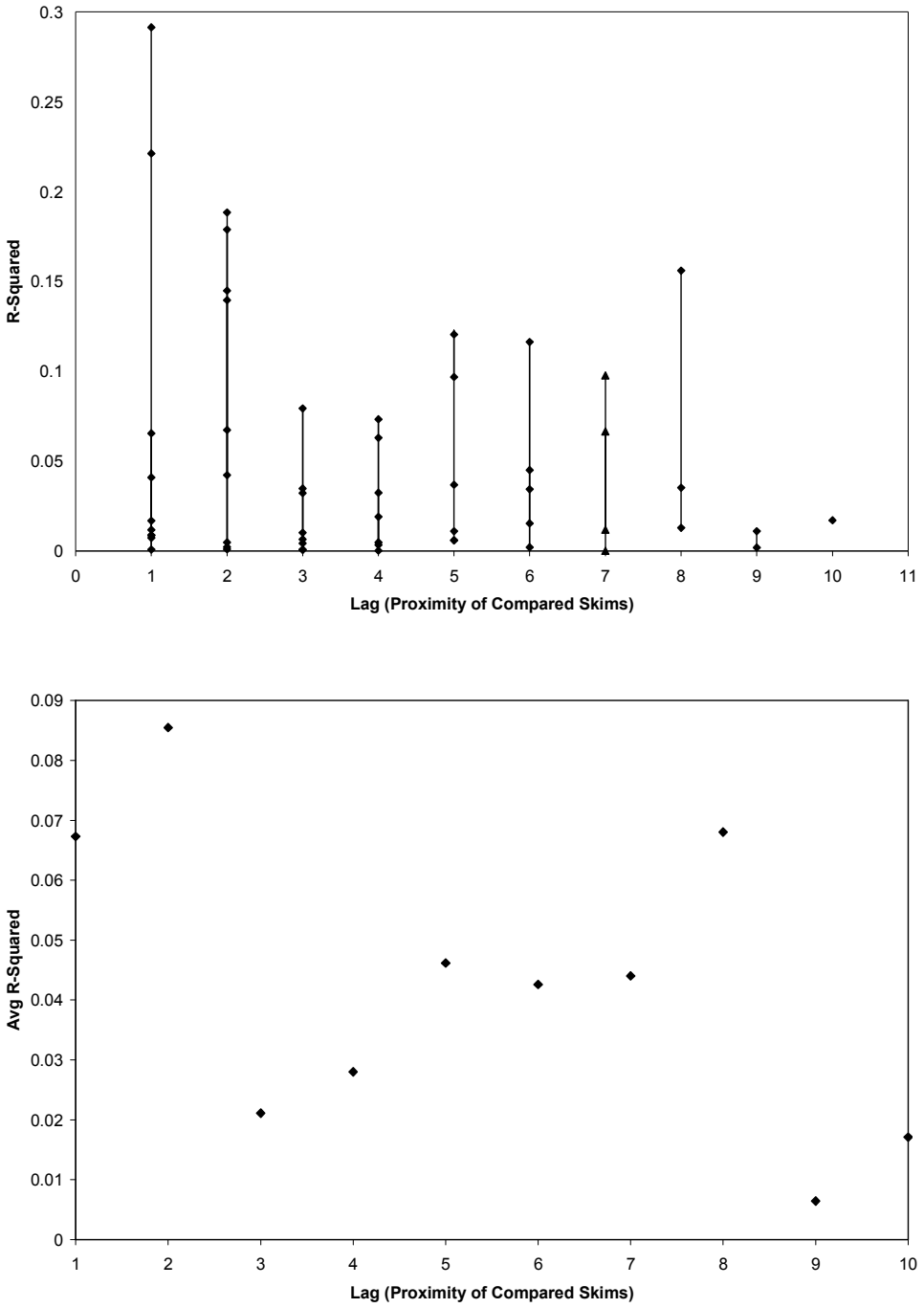

Figure 33. R-squared results for channel 16 EM amplitude analysis.

obtained from the .25 mm spacing. As with the previous analyses, linear regressions were calculated for each plot and R^2 values were found.

Amplitude Analysis Results

The analyses performed on the EM data produced some results (shown in Figures 30-33) that were expected and some that were not. The most interesting thing found from these data was the fact that, in each of the channels examined, the data correlated most strongly when compared to skims with a lag of one or two and then dropped off dramatically as the lag increased. This was expected for all of the instruments but was only found to be true for the EM values. The correlations that did exist, however, were significantly weaker than those seen in the magnetics data with the highest R^2 for each channel being around 0.1. This suggests that the data were organized in a predominantly random pattern.

EM Roughness

As a final procedure, a roughness analysis was performed to determine if the EM data were influenced by the topographic variations of the trench. To do this, an average of the 26 channels was calculated for each station resulting in one set of values for each skim. The same formula that was used for the magnetic roughness analysis was used to

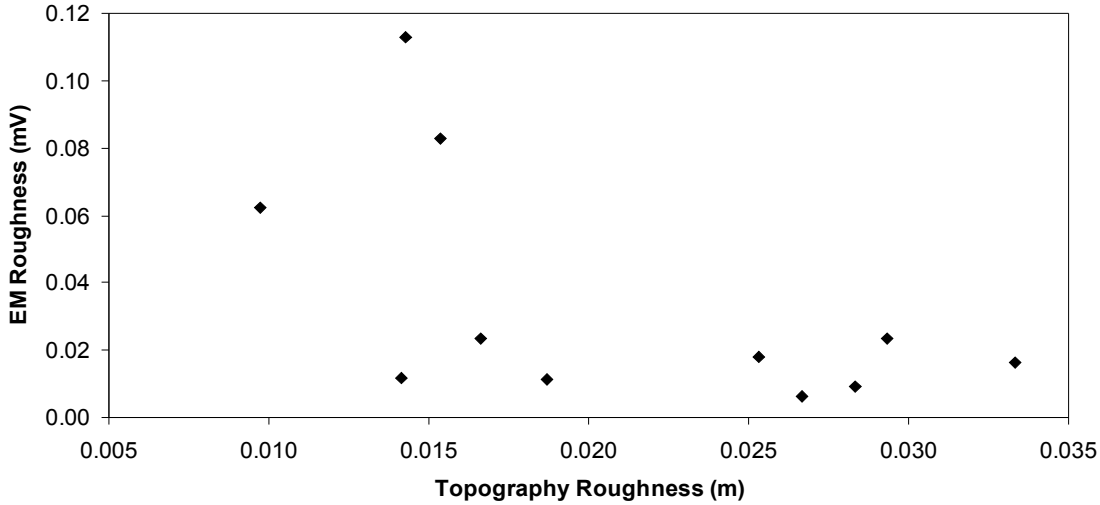

Figure 34. EM roughness vs. topographic roughness.

arrive at a single roughness value for each of the eleven skims. Those values were then plotted against the previously calculated topographic roughness values.

EM Roughness Results

The generated plots produced no evidence of a correlation between topographic variations and changes in the EM data (Figure 34). The data were distributed in a seemingly random fashion. A calculated R^2 of .33 was found, but it is believed that the apparent high level of correlation is due to the few number of data points that composed the plot.

CONCLUSIONS AND RECOMMENDATIONS

While this experiment yielded some findings consistent with the original hypothesis, many of the results of this research were unexpected. The first statement that can be made in conclusion is with respect to the influence of topographic variations along the survey line on the geophysical data. The data from this experiment have shown that there appears to be no effect on the acquired data resultant of topographic survey conditions. These results are favorable in that they suggest that no corrections need to be made to the data of the instruments used to account for elevation changes in a survey.

With respect to the effects of the soil removal on the response of each instrument, very little can be definitively stated. It was expected that there would be evident similarities in data compared from adjacent skims, with those similarities decreasing significantly as the skim lag increased. The data clearly show that this is not the case. The correlation values between the data from each instrument show little or no signs of decreasing as the lag of the compared skims increases. This suggests one of two possible scenarios. First, the majority of the geophysical signal is originating from the material that is removed by each subsequent skim, resulting in a completely different origin of the data for each skim. Secondly, the instrument data are resultant of heterogeneities sufficiently deep in the subsurface that the removal of the material throughout the experiment had no effect on the signal origin and, therefore, the datasets

from each skim were essentially the same as they were responding to heterogeneities located below the trench depth.

The data from this experiment do not provide enough evidence to suggest which of those two possibilities is more likely to be valid. Though much was learned by conducting this research, it is believed that much more can be understood about the nature of the origins of geophysical signals by learning from what was done both correctly and incorrectly in this experiment and applying that to a similar, but modified, experiment in the future.

A review of the procedures and operations resulted in the identification of three main factors that had adverse effects on the project. First, a better method of measurement along the survey line is needed. This experiment employed a flexible field tape measure that was fastened at the beginning and end of the survey line and had to be removed and replaced before and after each skim. In an attempt to maintain the same position, the tape was held tight which resulted in it being suspended over the skimmed area as the trench became deeper. This was undoubtedly the cause of inconsistencies in station location from one skim to the next. It would be beneficial to create permanent markers, either with survey paint or wooden stakes, located along the outer portion of the trench. These markers would not be in the path of the skimming process but would serve as control points along the survey line throughout the experiment.

Secondly, the experiment should be performed in an area with significant near-surface structure. The site chosen for this experiment was, in retrospect, too homogeneous to produce the desired results. While there were a number of signal

variances in each dataset resultant of subsurface heterogeneities, there were no features that could be coherently traced throughout the length of the survey area. It was later discovered that excavation training had at one time taken place near the experiment site leading to the possibility of that area being composed primarily of construction fill and not naturally deposited sediments. The presence of subsurface discontinuities in a natural environment would provide the heterogeneities necessary to produce significant signal variations from each of the instruments.

Finally, better control of the skimming process is essential. Though the material was removed as uniformly as could be expected using the given equipment, the amount of removal during each skim was inconsistent along the trench and resulted in an irregular surface. These irregularities were the source of problems primarily with GPR data collection, as the data are extremely sensitive to antenna orientation when a measurement is taken. A smooth trench floor is a necessity for acquiring data to be correlated for other skims.

REFERENCES

Atherton, W. A., 1980. The history of electromagnetic induction. American Journal of Physics 48 (9), 781-782.

Bano, M., 2004. Modeling of GPR waves for lossy media obeying a complex power law of frequency for dielectric permittivity. Geophysical Prospecting 52 (1), 11-26.

Basson, U., 1992. Mapping of moisture content and structure of unsaturated sand layers with ground penetrating radar. Tel-Aviv University, Israel.

Benavides, A., Everett, M.E., 2005. Target signal enhancement in near-surface controlled-source electromagnetic data. Geophysics 70, G59-G67.

Butler, D. K., 2003. Implications of magnetic backgrounds for unexploded ordnance detection. Journal of Applied Geophysics 54, 111-125.

Dalan, R. A., Bevan, B. W., 2002. Geophysical indicators of culturally emplaced soils and sediments. Geoarchaeology 17, 779-810.

Davis, J. L., Annan, A. P., 1989. Ground-penetrating radar for high-resolution mapping of soil and rock stratigraphy. Geophysical Prospecting, 37, 531-551.

Dobson, M. C., Ulaby, F. T., Hallikainen, M. T., El-Rayes, M. A., 1985. Microwave dielectric behavior of wet soil – Part II: Dielectric mixing models. IEEE Trans. Geosci. Remote Sens. 23, 35-46.

Everett, M.E., Weiss, C.J., 2002. Geological noise in near-surface electromagnetic induction data. Geophysics. Res. Lett. 29, 2001GL014049.

Gattacceca, J., Eisenlohr, P., Rochette, P., 2004. Calibration of *in situ* magnetic susceptibility measurements. Geophysical Journal International 158 (1), 42-49.

Hartsock, N. J., Mueller, T. G., Thomas, G. W., Barnhisel, R. I., Wells, K. L., Shearer, S. A., 2000. Soil electrical conductivity variability. Proceedings of 5th International Conference on Precision Agriculture. ASA Misc. Publ., ASA, CSSA, and SSSA, Madison, WI., 16-19.

Hendrickx, J. M. H., van Dam, R. L., Curtis, J., Lensen, H. A., Harmon, R., 2003. Worldwide distribution of soil dielectric and thermal properties. Detection and remediation technologies for mines and minelike targets VIII. Proceedings of the SPIE, Volume 5089, 1158-1168.

Lillie, R. J., 1999. Whole Earth Geophysics: An Introductory Textbook for Geologists and Geophysicists, Prentice Hall, Inc., Upper Saddle River, New Jersey.

Malliol, J., Ortega-Ramirez, J., Bernard, B., 2005. Archaeological feedback as a research methodology in near-surface geophysics. EOS Trans. AGU 86, Abstract NS41A-01.

McNeill, J. D., 1980a. Applications of transient electromagnetic techniques, Technical Note TN-7, Geonics Ltd, Mississauga, Ontario.

McNeill, J. D., 1980b. Electromagnetic terrain conductivity measurements at low induction numbers. Technical. Note TN-6, TN-8, Geonics Ltd, Mississauga, Ontario.

Milligan, P. R., Reed, G., 2004. Towards automated mapping of depth to magnetic/gravity Basement – examples using new extensions to an old method. ASEG 17th Geophysical Conference and Exhibition, Syndey, Australia, 1335-1355.

Nyquist, J.E., Boufadel, M.C., Doll, W.E., 2005. Advances in high-resolution magnetometry for mapping unexploded ordnance (UXO) and the challenge of geologic noise. EOS Trans. 86, Abstract GPR23A-02.

Sharma, P. V., 1997. Environmental and Engineering Geophysics, Cambridge University Press, Cambridge, England.

Smith, K., 1997. Cesium optically pumped magnetometers: Basic theory of operation, Technical Report M-TR91, Geometrics Inc, San Jose, CA.

Sun, J., Young, R.A., 1995. Recognizing cultural noise in ground penetrating radar data, Geophysics, 65, 5, 1378-1385.

Van Dam, R. L., Schlager, W., 2000. Identifying causes of ground-penetrating radar reflections using time-domain reflectometry and sedimentological analyses. Sedimentology 47 (2), 435-449.

Zoubir, A. M., Chant, I. J., 2002. Signal processing techniques for landmine detection using impulse ground penetrating radar. IEEE Sensors Journal 2 (1), 41-51.

VITA

Name:	Zachary Ryan Long
Address:	Department of Geology and Geophysics, Texas A&M University, College Station, TX 77843-3115
Email Address:	zlong@geo.tamu.edu
Education:	B.S., Petroleum Geology, The University of Louisiana at Lafayette, 2003